DEVELOPMENT OF A SMALL MOLECULE DRUG DELIVERY VEHICLE FOR TREATMENT OF CHRONIC PULMONARY DISEASES

A Thesis
Presented to
The Academic Faculty

By

Megan Christina Lofton

In Partial Fulfillment
of the Requirements for the Degree
Master of Science in the
School of Biomedical Engineering

Georgia Institute of Technology
Emory University
August 2008

DEVELOPMENT OF A SMALL MOLECULE DRUG DELIVERY VEHICLE FOR TREATMENT OF CHRONIC PULMONARY DISEASES

Approved by:

Dr. Thomas Barker, Advisor
Department of Biomedical Engineering
Georgia Institute of Technology

Dr. Niren Murthy
Department of Biomedical Engineering
Georgia Institute of Technology

Dr. Jesse Roman
Department of Pulmonology
Emory University

Date Approved: 06/08

To my Jive Turkey, your support was everything…

ACKNOWLEDGEMENTS

Thank you Thank you Thank you God for seeing me through! With your grace I was able to accomplish what many times I thought was the impossible…..

Also, I would like to thank the many people that made it possible for me to complete this thesis. Without each and every one of your generous spirits I don't know where I would have been. Specifically, I'd like to express supreme gratitude to Stephen for his expertise in particle synthesis and in all the hardships related, Scott and Sungmun for their help as well, and all of those in the Murthy lab that opened the door for me time after time. In the Roman lab, I would like to thank Susanne for her over whelming willingness to aid me in the biocompatibility studies. She displayed great dedication, even to the point of resuscitating mice on their deathbeds. Also, Jeff thank you. Your guidance was irreplaceable. I'd like to give a special thanks to Hilda for her help as well. In addition, thank you Edilson for giving me an overview in histology 101. Thank you to Allyson, Ashley, Cedric, Sarah, and formerly Nikki, my lab, for being there to support me. Thank you for being my sounding board and at times source for new direction and ideas. And to Ruby, you didn't understand a word, but somehow telling you made everything clear. I miss you so much, everyday. And my friends and family deserve thanks. You were sometimes a distraction, but I know you are proud and wanted to help me in this accomplishment. Thank you Shannon Sullivan for keeping me apprised of all those numerous deadlines. Also, I extend much appreciation to my committee members Drs. Murthy and Roman. Lastly, but not least thank you Dr. Barker for respecting and supporting my academic choices allowing me to pursue my desires without wasting what I started.

TABLE OF CONTENTS

LIST OF TABLES

LIST OF FIGURES

SUMMARY

Lung disease claims nearly half a million lives in the U.S. alone, placing it as the third leading cause of death. Chronic pulmonary disorders, marked by excessive extracellular matrix deposition (ECM), such pulmonary fibrosis, are the most resistant to present clinical therapies resulting in prognoses of 50% life expectancy three years from diagnosis. Inadequacies of current treatments may be attributable to limitations in non-invasive therapeutic administration modalities. However, with the use of polyketal microparticles (PKMs), a novel drug delivery vehicle, a myriad of therapeutic schemes may be explored. Polyketals are a new polymeric family characterized by excellent tissue biocompatibility, rapid hydrolysis, and benign degradation byproducts making it attuned for pulmonary applications. Potential treatments such as siRNA, oligo nucleotides, peptides, enzymes and other biomolecules can be encapsulated within PKMs and administered non-invasively via inhalation.

For this study, we selected a model therapeutic peptide, Ac-SDKP, with established anti-fibrotic properties as the “load” for PKMs. For those lung dysfunctions characterized by pathological ECM remodeling accompanied by fibrotic scarring, Ac-SDKP possesses promise in restoring the normal ECM framework. To assess PKMs viability as a pulmonary drug delivery vehicle three objectives were initially defined: 1) Synthesize particles possessing aerodynamic properties conducive for aerosolization with low polydispersity, 2) Optimization of the therapeutic load, Ac-SDKP, in PKMs to levels that will translate to reasonable clinical dosing concentrations, and 3) Determine the biocompatibility of the PKMs in the lung.

Optimization of the Ac-SKDP loading within PKMs and size analysis revealed that a solid in oil in water double emulsion particle synthesis technique produced the most ideal microspheres. Based on previous reports, the loading efficiency attained,

when locally dispensed into the alveolar space, should reach clinical dosing requirements. Synthesized particles were compatible with aerosolization criteria; i.e., diameters below 3 μm and low polydispersities. The relatively low particle size distributions should promote uniform particle dissemination and hydrolysis allowing therapeutic release to be consistent. In addition, we evaluated PKM tissue biocompatibility using a murine lung model. Examination of bronchoalveolar lavage fluid demonstrated only a slight inflammatory response to intratracheal particle injections of PKMs whereas PLGA, a commonly used biomaterial, elicited a significantly higher response. Histological assessment of the lungs following particle injection verified PKMs' biocompatibility superiority. In conclusion, small-diameter PKMs (1-3 μm) are a suitable delivery system for pulmonary drug delivery, capable of delivering small peptide therapeutics and evading the local inflammatory response. The present work will enable expansion of therapeutic avenues capable of combating chronic lung disease.

CHAPTER 1

INTRODUCTION

1.1 Background and Significance

Displaying increasing incidence, lung disease is the third leading cause of death resulting in over 350,000 American fatalities annually**.** Significant contributions to pulmonary disease morbidity are those classified as chronic lung disease in which 35 million U.S. citizens are afflicted (American Lung Association). This class of lung pathology includes common disorders such as chronic obstructive pulmonary disease (COPD) (i.e. chronic bronchitis and emphysema), bronchopulmonary dysplasia (BPD), and interstitial lung disease (ILD). Although, the onset of these disorders is diverse, all are characterized by incurable compromised lung function largely due to pathological tissue remodeling. The pathophysiology of these chronic lung diseases often result in fibrotic scarring and stiffening of pulmonary structures that disrupt essential respiratory processes. Resultant clinical symptoms can manifest as shortness of breath, wheezing, severe cough, and low blood oxygen levels (American Lung Association). With lung disease prevalence failing to diminish, it is evident the efficacy of standard clinical treatments is inadequate.

Management techniques of certain chronic lung diseases have higher success than others, but none are considered a cure. For instance BPD, a disease characterized by lung inflammation and scarring in premature infants, can be partially resolved with current treatments (Ashour et al. 2006). This can include high oxygen therapy, use of bronchodilators and low-pressure lung ventilation systems. These treatments solely focus on supporting the oxygen needs of the infant while symptoms of the BPD subside as the child develops. However, they do little to combat the source of the lung dysfunction resulting in gradual, incomplete recovery (Jobe 1999). Current treatments of

COPD also include oxygen therapy, use of bronchodilators as well as inhalable corticosteroids to treat inflammation. Again, the pathophysiology of the disease causing airflow restriction and lung tissue remodeling is not effectively addressed (Barnes 2000). This can potentially lead to survival projections only of ten years if diagnosis and treatment is delayed. Perhaps, the most resistant of all to current treatments is interstitial lung disease or more specifically pulmonary fibrosis. This disease, marked by progressive lung scarring and stiffening, causes up to 50,000 American deaths each year. To date, there exists no therapeutic that impedes the advancement of the disease or averts its onset. As a result, pulmonary fibrosis has one of the gravest prognoses with 50% life expectancy 3 years from diagnosis.

In general, current treatments for chronic lung diseases focus on alleviating the symptoms and not the source of the ailment. This potentially is due to limiting therapeutic administration modalities. Currently, therapies are restricted to oral supplements, intravenous routes, or medications capable of achieving an inhalable form. Oral and intravenous modes of treatment leave patients susceptible to undesirable systemic side effects especial with routinely used immunosuppressing corticosteroids (Mapel, D.W. et al. 1996). With a novel delivery system, varieties of locally dispensed therapeutic schemes can be expanded, substantially minimizing risk of systemic side effects. Utilizing polyketal microparticles as a drug delivery vehicle, vast strides can be made with treatments of lung diseases, especially pulmonary fibrosis. Polyketal microparticles (PKMs) are composed of a biocompatible, biodegradable polymer capable of encapsulating small molecule therapeutics, allowing for a controlled release of drug while minimizing the induction of inflammation (Dailey, L.A., et al 2006). Appropriately sized, in the range 1-3 um for non-porous particles, PKMs have the potential to be delivered to the alveolar space through non-invasive techniques such as

inhalation (Cryan, S.A. 2005). Use of PKMs could permit delivery of siRNA, enzymes, oligo nucleotides, small peptides or other promising therapeutics that would otherwise be degraded too quickly to be effective, face difficulties with effective local delivery or have undesirable side effects if administered systemically. By utilizing these particles, chronic lung diseases can be targeted on the cellular and nuclear level in a tunable and sustained fashion.

1.2 Objectives

The goal of this study is to demonstrate that polyketal microparticles are effective as a drug delivery vehicle specified for pulmonary applications. To achieve this goal, as a proof of principle, a representative therapeutic was chosen to encapsulate within the polyketal microparticles that could have promise in the treatment of a chronic lung disease. The small hydrophilic peptide, Ac-SDKP, which has been shown to have anti-fibrotic properties in heart and kidney tissues, was ideal due to its potential to combat the currently untreatable pulmonary fibrosis (Yang, F., et al. 2004). To assess the value of polyketals as a drug delivery vehicle our study included three objectives. 1) Synthesize porous 10-20 um or non-porous 1-3 um particles with low polydispersity. 2) Optimize the load of the representative therapeutic, Ac-SDKP, in the polyketal microparticles to levels that will translate to reasonable clinical dosing concentrations. 3) Determine the biocompatibility of the polyketal particles in the lung using a murine model.

1.3 Hypothesis

Our central hypothesis is that polyketal particles do not elicit a significant inflammatory response in the lung and can be synthesized and optimally loaded with the potential anti-fibrotic therapeutic, Ac-SDKP.

CHAPTER 2

LITERATURE REVIEW

2.1 Inadequacies of Current Chronic Lung Disease Treatments

Symptoms commonly associated with chronic lung diseases such as labored breathing and low blood oxygen levels are attributable to the pathological alterations of normal pulmonary structures. COPD, BPD, and pulmonary fibrosis all have a unifying, salient feature of exhibiting inflammation followed by deposition of fibrotic tissue or scars. The initiation of inflammatory responses may vary among disease states and includes triggers such as environmental irritants, ventilator injury, genetic cues, or is simply idiopathic (Crouch 1990). However, as inflammation facilitates fibrosis, all can be histologically characterized by excessive extra cellular matrix (ECM) deposition largely due to increased fibroblastic proliferation (Gay, S.E., et al. 1998). The exact mechanism of the accumulation of fibrotic tissue has not been fully elucidated, but it is clear that this pathological remodeling response to lung injury is the source of compromised pulmonary functionality. Clinical management of these lung disorders has generally been ineffective at addressing the source of pulmonary dysfunction. The efficacy of bronchodilators and corticosteroids in COPD and pulmonary fibrosis has been extremely limited (Barnes 2000). Furthermore, systemic use of these agents leaves patients vulnerable to side effects such as brittle bones, cataracts, immunosuppression, tachycardia, and muscle tremors. A therapeutic that addresses the abnormal ECM framework has yet to be discovered, which presumably would lead to optimal lung function.

Since many chronic lung diseases are progressive, a potent therapeutic scheme necessitates non-invasive, directed administration. For disease states involving a long-term surplus of ECM accumulation resulting in fibrosis, such therapies would be beneficial, facilitating sustained or multi-coursed therapy. With fibrotic pathologies,

fibroblasts, cells primarily responsible for ECM production, are in a heightened proliferative state. In addition, the ECM within established fibrotic scars is not as readily degraded as normal ECM. The combination of these phenomena leads to the chronic and progressive nature of these disease states. This highlights the pertinence of the development of therapies locally and non-invasively dispensed, so that the treatment maintains efficacy and longevity while minimizing side effects.

2.2 Polyketal Microparticle Benefit in Pulmonary Drug Delivery

With insufficient current treatments for chronic fibrotic lung disorders, an optimal treatment strategy is delivery of a therapeutic capable of retarding disease progression, without exacerbating the inflammatory response. Polymeric microparticles have been explored as a platform to non-invasively direct treatments to the lung interstitium. However, certain design criteria must be achieved in order for microparticles to be a viable option for lung drug delivery. Sized in the range of 1-3 um or 10-20 um for porous microparticles, these biomaterials have the potential to be inhaled comfortably by a patient from a dry powder spinhaler (Edwards, D.A., et al 1997). Once inhaled, the drug-encapsulated microparticles will be deposited in the alveolar regions of the lung (Arnold, M.M., et al. 2007). The therapeutic potency can be further maximized through encapsulation in microparticles with short half-lives and excellent biocompatibility. This type of delivery allows for multiple, patient controlled, sustained administrations of treatment, which may prove beneficial in combating the progressive nature of these lung diseases.

Presently, use of micoparticles as delivery vehicles to the lung have failed due to inadequacies of current biomaterials to be both aerosolizable and biocompatible. Ideally, microparticles are composed of hydrophobic polymers in order to prevent particle aggregation, which could disrupt the particle aerosolization process. Therefore,

biocompatible materials such as alginate are not suitable for drug delivery because its hydrophilicity leaves it prone to aggregation. Another polymer, PLGA (Poly (dl-lactide/glycolide)), while hydrophobic and possessing structural properties necessary to form aerosolized particles, has been shown to elicit significant inflammatory responses. Previous studies in hamsters have demonstrated PLGA's poor biocompatibility in the lung. Results indicated that following a 1 mg intratracheal dose of 1-2.4 um PLGA micoparticles, macrophage populations increased 8 fold and neutrophil infiltration amplified by a factor of 20 within 24 hrs. Coupled with this, increased lymphocyte influx required 10 days to subside (Springer, C., et al. 2005). PLGA's acidic degradation products perpetuate activation of immune and inflammatory cells. Upon PLGA hydrolysis, pH values can reach as low as 2-3, which not only exacerbates inflammation, but can potentially destabilize encapsulated biomolecules and/or catalyze inadvertent reactions (Houchin, M.L. et al. 2006). Another, undesirable property of PLGA is its extended half-life of approximately 40 days. Slow degradation of the particles impedes the release of active therapeutic and particle accumulation would preclude possibilities of frequent dosing (Dailey, L.A., et al. 2006). This would likely thwart the capabilities of the delivered drug to combat the persistent progression of these lung abnormalities.

However, a new polymer has emerged that possesses promise in addressing challenges encountered by other polymer formulations. Polyketal polymers were developed based on an acetal exchange reaction (Lee, S., et al. 2007), which results in a polymer structure containing a ketal linkage in its backbone (Heffernan, M.J. and N. Murthy 2005). Such a chemical structure generates the benign hydrolysis products, acetone and diols. Acetone and diols are both neutral byproducts in contrast to PLGA's acidic degradation products, which should not induce a significant inflammatory response. According to preliminary studies, polyketal microparticles injected at high doses into muscle do not inflame tissues. Concomitantly, potential for inflammatory cell

activation is further reduced by the short 2-day half-life of certain polyketals at pH 4.5. Degradation products are membrane permeable, which will facilitate timely clearance from the lung following phagocytosis. This property will allow for frequent, multi-coursed therapies because particles should not accumulate in the lung in contrast PLGA particles. In addition, polyketals are hydrophobic and therefore possess the traits necessary to resist aggregation permitting aerodynamic properties to remain optimal for inhalation.

Polyketal formulations are versatile and polymer properties such as hydrolysis rates can be manipulated to address specified applications. Previously, two other formulations of polyketals have been investigated for drug delivery, poly-(1,4-phenyleneacetone dimethylene ketal) (PPADK) and poly(cyclohexane-1,4-diyl acetone dimethylene ketal) (PCADK). However, these polyketals are not ideal for lung delivery and treatment of fibrotic disorders. PPADK has a rapid half-life of 35 hours at pH 5, but degrades into toxic aromatic byproducts (Heffernan, M.J. and N. Murthy 2005). PCADK has superior biocompatibility, but a long half-life of 24 days at pH 4.5 (Lee, S., et al. 2007). Based on PCADK's established biocompatibility, for the present study a PCADK derivative was used called PK3. This formulation exhibits a vastly decreased half-life of 2 days at pH 4.5, while maintaining biocompatibility. PK3 is comprised of 87 mole% cyclohexane dimethanol and 13 mole% pentane diol and possesses many of the attributes required to be an effective carrier of therapeutics for pulmonary applications.

2.3 Ac-SDKP Potential As an Anti-fibrotic Agent For Chronic Lung Diseases

The exact mechanisms governing excess ECM deposition and the pathological remodeling of pulmonary structures observed with many chronic lung disorders remains unknown. However, key factors have been identified that significantly influence the progression of fibrotic disorders in animal models. Previous research has suggested that

the Transforming Growth Factor-beta (TGF-ß) signaling cascade may be the crux of these fibrotic pathologies (Gauldie, J., et al. 2007). The vast majority of TGF-ß exists in an inactive form and is bound to the latency-associated protein (LAP). Once TGF-ß is activated (partially or fully) by chemical or mechanical detachment of LAP, it is free to assert action upon its cell surface receptors. TGF-ß type I and II receptors following stimulation, initiate an intercellular signaling cascade that leads to the phosphorlation of the receptor activated Smads, smad 2 and 3. Phosphorlated smad 2/3 then complex with smad 4 and proceed to translocate to the nucleus where they direct gene expression as transcription factors (Gauldie, J., et al 2007). Many of the downstream effects of TGF-ß activation include the production and secretion of ECM proteins (Verrecchia, F. and A. Mauviel 2004) as well as alveolar epithelial to mesenchymal cell transition, which has been proposed to increase the number of ECM secreting cells (Kasai, H., et al. 2005). In pathological states involving fibrosis this pathway appears to be over activated and uncontrolled leading to increased deposition of ECM, which consequently stiffens the lung and promotes dysfunction. Animal models of pulmonary fibrosis have demonstrated that TGF-ß mRNA is upregulated in macrophages, which after secretion likely inundates the TGF-ß cascade resulting in eventual fibrotic effects (Higashiyama, H., et al. 2007). However, present studies indicate that prevention of some fibrotic models can be achieved by utilizing function-blocking antibodies against TGF-ß or soluble decoy TGF-ß receptors (Scotton, C.J. and R.C. Chambers 2007). Based on these results, it appears that a promising therapeutic would target disruption of the TGF-ß signaling pathway.

Recently, the endogenous peptide seryl-lysyl-aspartyl-proline (SDKP), has been investigated as an anti-fibrotic agent potentially capable of regulating over activated TGF-ß responses. SDKP is the proteolytic byproduct of thymosin ß4 (Cavasin, M.A., et al 2004) and was first identified in context to the rennin-angiotensin system in the

regulation of systemic blood pressure as it is readily degraded by angiotenisin converting enzyme (Azizi, M., et al. 1997). In addition, SDKP has been shown capable of arresting some cells such as fibroblasts and hematopoietic stem cells in the S-phase, therefore halting proliferation (Rhaleb, N.E., et al 2001, Cashman, J.D.et al. 1994). Other studies have revealed that decreased levels of circulating SDKP initiate multi organ fibrosis (Cavasin, M.A., et al. 2007) while administration of SDKP post-infarct diminishes inflammation and fibrotic tissue accumulation absent of adverse blood pressure effects (Yang, F., et al. 2004). On the protein level, SDKP further exhibits anti-fibrotic effects through inhibition of endothelin1 facilitated collagen expression (Rhaleb, N.E., et al 2001). Even more relevant are the indications that SDKP elicits an efflux of smad 7 from the nucleus, resulting in interference of the TGF-ß signaling cascade. Specifically, smad 7 acts as a regulator and complexes with smad 2/3 preventing it from associating with smad 4. Without smad 4 association, gene transcription due to TGF-ß signaling through the smad pathway is diminished (Kanasaki, K., et al. 2006). SDKP has been shown to inhibit fibrotic events through multiple pathways on the nuclear, protein and organismal levels. Therefore, its use for treatment of chronic lung diseases characterized by fibrosis has great potential.

2.4 Conclusion

Current treatments of many chronic lung diseases have remained futile, failing to address the root of lung dysfunction. Typical approaches include the use of bronchodilators and corticosteroids, which do little to combat pathologies characterized by significant fibrosis. Thus far, administration of potential therapeutics has been restricted to oral supplements, intravenous routes, or medications capable of achieving an inhalable form. However, by utilizing polymeric micoparticles as a drug delivery vehicle, numerous therapeutics have the potential to deposited in the alveolar space

through simple inhalation. Polyketal microparticles, more specifically PK3, have been shown to exhibit properties attuned with pulmonary drug delivery such as biocompatibility and short half-lives. They have the capacity to encapsulate a variety of biomolecules such as siRNA, enzymes, oligo nucleotides and small peptides that could be investigated for efficacy in treating pulmonary complications. In this study, PK3's viability as a pulmonary drug delivery vehicle was assessed using the model therapeutic Ac-SDKP. Ac-SDKP, from previous studies, asserts an anti-fibrotic effect through the disruption of the TGF-ß signaling cascade, which is an established facilitator of pulmonary fibrosis. By determination of biocompatibility and optimization of encapsulation of this model drug, PK3 microparticles have the potential to reveal novel therapeutic avenues that address the inadequacies of present clinical treatments of chronic lung diseases.

CHAPTER 3

AC-SDKP LOADED POLYKETAL PARTICLE SYNTHESIS OPTIMIZATION AND CHARCTERIZATION

3.1 Introduction

Ideally, effective therapeutic carriers for pulmonary applications can be efficiently loaded with a target therapeutic, while maintaining specified size constraints. The synthesized particles should display low polydispersity and sizes in the range of 1-3 um for non-porous particles and 10-20 um for porous particles (Cryan, S.A 2005, Sung, J.C. 2007). These size constraints ensure drug release is uniform and preservation of aerodynamic properties. Preliminary studies indicate that non porous particles ranging from 0.5–4.14 um can be effectively aerosolized and dispersed, which is necessary for particle inhalation. In addition, optimal Ac-SDKP loading will minimize the eventual particle dosing required for clinical applications of the therapeutic and concurrently minimize the risk of inflammatory or immune responses due to the particles.

In an effort to satisfy the prescribed particle design criteria, various double emulsion particle synthesis techniques were evaluated according to the drug load efficiency and particle size distribution. Double emulsions are essential for encapsulation of hydrophilic molecules (e.g. Ac-SDKP) within hydrophobic polymers (e.g. PK3) due to the low affinity the peptide has for the polymer. The basic water in oil in water (w/o/w) double emulsion technique involved solubilizing the peptide within a surfactant containing solution such as poly vinyl alcohol (PVA), which increased the peptide's probability of interaction with the polymer. Then emulsifying the peptide solution within an organic solution containing PK3 yielded the primary emulsion. After which, a more concentrated surfactant solution was added to the primary emulsion and subsequently emulsified again. This caused the PK3 to form microspheres encompassing the previously emulsified peptide. By immediately evaporating the organic solvent from the

particle suspension, the microparticles were allowed to harden and stabilize. At this stage, microparticles were washed free of PVA and dried by lyophilization.

We altered various parameters in this basic w/o/w double emulsion synthesis technique in an attempt to address our objective of optimally loading Ac-SDKP within polyketal particles. First, the emulsion apparatus of both the primary and secondary emulsion were varied with the goal of controlling particle size distribution without diminishing drug load efficiency. The rationale was that the more rigorous the agitation process, the smaller and narrower the size distribution of the resulting particles. Secondly, the effect of the outer aqueous phase (i.e. the surfactant solution of the secondary emulsion) pH was investigated. Based on previous work, a pH similar to the isoelectric point (pI) of the drug of interest increased load efficiency (Peltonen 2004). For Ac-SDKP, the pI is approximately 5.55 and when exposed to solutions of this pH the peptide maintains a neutral charge, which should facilitate its encapsulation within the hydrophobic polyketal. Thirdly, the drug to polymer ratio of the initial formulation was altered in an effort to increase load efficiency. Studies, based on work by Peltonen et al., have indicated that using minimal drug to polymer ratios promote optimal drug encapsulation (Peltonen 2004).

In addition to the aforementioned parameter perturbations, we further modified the double emulsion by utilizing a cryo w/o/w emulsion and a solid in oil in water emulsion (s/o/w). The cryo w/o/w emulsion method involved freezing the primary emulsion before performing the secondary emulsion. This method attempted to slow the release of the peptide into the outer aqueous phase due to the peptide's frozen state at the commencement of the secondary emulsion. Theoretically, this method will increase drug entrapment within formed microparticles. The s/o/w technique capitalized on the peptide's insolubility in organic solvents. After solid peptide dispersion within the primary emulsion via sonication, the secondary emulsion was performed. For peptide loss to

occur, it must first dissolve in the aqueous phase. The lengthened time required to solubilize the peptide permits the peptide to remain in the organic phase longer and thus increases the likelihood a polymeric microparticle will encapsulate the peptide.

After optimally loading microspheres, we further characterized the particles by assessing preservation of the encapsulated therapeutic's bioactivity. From this assessment we determined the effect processing these loaded microparticles has on the capacity of Ac-SDKP to function as an anti-fibrotic agent. Previous studies have established that Ac-SDKP, administered *in vitro*, can down regulate TGF-ß induced Fibronectin (FN) mRNA expression (Guo et al. 2004, Hocevar et al.1999). Therefore, by stimulating cells with TGF-ß to promote FN expression and subsequently treating cells with Ac-SDKP loaded particles, bioactivity can be quantitatively compared by resultant FN mRNA levels. By systematically exploring the effects of these specified particle synthesis parameters, Ac-SDKP loading was optimized and fully characterized.

3.2 Methods

3.2.1 Materials

PK3 polymer (generously donated by Murthy lab), Ac-SDKP peptide (Genscript, Piscataway, NJ), fluorescamine (MP Biomedicals, Solon, OH), acetone (VWR International, Suwanee, GA), chloroform (EMD Chemicals, Cincinnati, OH), polyvinyl alcohol (Aldrich, St. Louis, MO), diochloromethane (ACROS, Geel, Belgium), hexane (ACROS, Geel, Belgium), primary rat lung Sprague Dawley (RLSD) fibroblasts (isolated by Ashley Carson), Dulbecco's Modification of Eagle's Media (Mediatech, Herndon, VA), Fetal Bovine Serum (Mediatech, Herndon, VA), Penicillin-Streptomycin (Mediatech, Herndon, VA), RNeasy Kit (Qiagen, Valencia, CA), Power SYBR Green I RNA to Ct Kit (Applied Biosystems, Foster City, CA), Fibronectin qPCR primers (Invitrogen, Frederick, Maryland), B-actin qPCR primers (Occam Biolabs, Newark, DE).

3.2.2 Ac-SDKP Loaded PK3 Particle Synthesis Optimization

3.2.2.1 Basic Double Emulsion Technique

Ac-SDKP peptide (5 mg) was dissolved in 50 ul of a 1% (v/v) polyvinyl alcohol solution (PVA) at pH 8.5 to yield a 100 mg/ml peptide solution. The peptide solution was added to an 8 ml glass vial. In a separate 8 ml glass vial, 50 mg of PK3 was dissolved in 500 ul of dichloromethane (DCM) to also yield a 100 mg/ml solution. The PK3 in DCM solution was then added to the Ac-SDKP peptide solution and emulsified with a probe sonicator for 30 sec (output 20W). Immediately, 5 ml of a 5% PVA buffered (pH 6.8) solution was added to this primary emulsion and homogenized (level 2) for 1.5 min yielding the secondary emulsion. The emulsion was added to a 100 ml round bottom flask and DCM was removed with the use of a Rotovap. The flask was rotated at speed 3 for the duration of the evaporation process, which included cycling the mixture between low and high pressures over the course of approximately 10-15 min. Contents of the 100 ml round bottom flask (particle suspension) were then dispensed into a 15 ml conical tube and diluted with deionized water to approximately 10 ml. A 1 ml aliquot of the particle suspension was reserved for dynamic light scattering analysis to determine particle size distributions. The particle suspension was centrifuged for 10 min at 6000xg. The supernatant was removed and particles resuspended by vortexing with 10 ml of fresh deionized (DI) water to remove PVA. Centrifugation was repeated. The supernatant was again removed and the particles resuspended with fresh DI water. The suspension was then frozen for approximately 45 min at -80 C. The frozen particle suspension was lyophilized overnight.

3.2.2.2 Emulsion Apparatus Optimization

The particle synthesis was performed according to the previous basic technique protocol with the exception of varying the emulsion devices for the primary and

secondary emulsions. Perturbations of the parameters are listed below (Table 1). Three experiments were performed and the basic particle synthesis technique conditions as detailed previously are highlighted in blue.

Table 1. Emulsion Devices.

Exp't. No.	**Primary Emulsion**		**Secondary Emulsion**	
	Device	Time	Device	Time
A1	Sonicator	30 sec	Homogenizer (speed 2)	90 sec
A2	Homogenizer (speed 2)	90 sec	Vortex (3000 rpm)	120 sec
A3	Sonicator	30 sec	Vortex (3000 rpm)	120 sec

3.2.2.3 Outer Aqueous Phase pH Optimization.

The particle synthesis was performed according to the previous basic technique protocol with the exception of varying the outer aqueous phase pH (i.e. the pH of the 5% (v/v) PVA solution of the secondary emulsion). Perturbations of the parameters are listed below (Table 2). Four experiments were performed and the basic technique conditions are highlighted in blue.

Table 2. pH of Outer Aqueous Phase.

Exp't. No.	**5% PVA pH**
B1	6.8
B2	11.1
B3	5.3
B4	1.2

3.2.2.4 Drug to Polymer Ratio Optimization

The particle synthesis was performed according to the previous basic technique protocol with the exception of varying the drug to polymer ratio in the initial formulation. Perturbations of the parameters are listed below (Table 3). Two experiments were performed and the basic technique conditions are highlighted in blue.

Table 3. Drug to Polymer Ratio. Note: Basic technique experimental conditions were not performed again.

Exp't. No.	**SDKP: PK3**
Basic Tech.	10% (add 50 ul of 100 mg/ml SDKP)
C1	5% (add 25 ul of 100 mg/ml SDKP)
C2	15% (add 75 ul of 100 mg/ml SDKP)

3.2.3 Ac-SDKP Loaded Porous Particle Synthesis

A particle synthesis technique ensuring the fabrication of porous particles was performed. In a 4 ml glass vial, 15 mg of Ac-SDKP peptide was dissolved in 150 ul of 1% (v/v) PVA pH 8.5 resulting in a 100 mg/ml peptide solution. Then in an 8ml glass vial, 150 mg of PK3 was in dissolved in 1375 ul of DCM + 225 ul of hexane by vortexing and heating. The 100 mg/ml Ac-SDKP solution was pipetted into the bottom of the 8 ml glass vial containing the PK3, DCM, and hexane. This mixture was homogenized for 1.5 min. at speed 5 yielding the primary emulsion. Next, this primary emulsion was pipetted into the bottom of 20 ml of a 5% (v/v) PVA (buffered). This mixture was again homogenized for 1.5 min, at speed 2. Immediately, this secondary emulsion was poured into 80 ml of 1% (v/v) PVA. The resulting mixture was placed on the Rotovap in a 500 ml round bottom flask to the remove the organic solvents. The flask was rotated at speed 3 without heat for 15 min to remove the DCM. Subsequently, the flask was submerged in a 30 C water bath while continuing to rotate at speed 3 for an additional

30 min to remove the hexane. After the organic solvent removal, a 1 ml aliquot of the particle suspension was reserved for dynamic light scattering (DLS) analysis. The remainder of the particle suspension was divided into two 50 ml conical tubes. The suspensions were then centrifuged at 8000xg for 10 min. The supernatant was removed and particles resuspended by vortexing with 10 ml of fresh deionized (DI) water to remove PVA. Centrifugation was repeated. The supernatant was again removed and the particles resuspended with fresh DI water. The suspension was then frozen for approximately 45 min at -80 C. Frozen particle suspension was lyophilized overnight.

3.2.4 Solid in Oil in Water Double Emulsion

Solid Ac-SDKP peptide (5 mg) was added to an 8 ml glass vial. In a separate 8 ml glass vial, 50 mg of PK3 was dissolved in 400 ul of dichloromethane (DCM) and 100 ul ethyl acetate to also yield a 100 mg/ml solution. The PK3 in DCM/ ethyl acetate solution was then added to the solid Ac-SDKP peptide and emulsified with a probe sonicator for 30 sec (output 20 W). Immediately, 5 ml of a 5% PVA buffered (pH 6.8) solution was added to this primary emulsion and homogenized (level 3) for 1.5 min yielding the secondary emulsion. The emulsion was added to a 100 ml round bottom flask and DCM was removed with the use of a Rotovap. The flask was rotated at speed 3 for the duration of the evaporation process, which included cycling the mixture between low and high pressures over the course of approximately 10-15 min. Contents of the 100 ml round bottom flask (particle suspension) were then dispensed into a 15 ml conical tube and diluted with deionized water to approximately 10 ml. A 1 ml aliquot of the particle suspension was reserved for dynamic light scattering analysis to determine particle size distributions. The particle suspension was then centrifuged for 10 min at 6000xg. The supernatant was removed and particles resuspended by vortexing with 10 ml of fresh deionized (DI) water to remove PVA. Centrifugation was repeated. The

supernatant was again removed and the particles resuspended with fresh DI water. The suspension was then frozen for approximately 45 min at -80C. Frozen particle suspension was lyophilized overnight.

3.2.5 Cryo Water in Oil in Water Double Emulsion

Ac-SDKP peptide (5 mg) was dissolved in 50 ul of a 1% (v/v) polyvinyl alcohol solution (PVA) at pH 8.5 to yield a 100 mg/ml peptide solution. The peptide solution was added to an 8 ml glass vial. In a separate 8 ml glass vial, 50 mg of PK3 was dissolved in 500 ul of dichloromethane (DCM) to also yield a 100 mg/ml solution. The PK3 in DCM solution was then added to the Ac-SDKP peptide solution and emulsified with a probe sonicator for 30 sec (output 20W). Then this primary emulsion was frozen completely in a dry ice/ acetone mixture. Immediately after freezing, 5 ml of a 5% (v/v) PVA buffered (pH 6.8) solution was added to this primary emulsion and homogenized (speed 3) for 1.5 min yielding the secondary emulsion at room temperature. The emulsion was added to a 100 ml round bottom flask and DCM was removed with the use of a Rotovap. The flask was rotated at speed 3 for the duration of the evaporation process, which included cycling the mixture between low and high pressures over the course of approximately 10-15 min. Contents of the 100 ml round bottom flask (particle suspension) were then dispensed into a 15 ml conical tube and diluted with deionized water to approximately 10 ml. A 1ml aliquot of the particle suspension was reserved for dynamic light scattering analysis to determine particle size distributions. The particle suspension was centrifuged for 10 min. at 6000xg. The supernatant was removed and particles resuspended by vortexing with 10 ml of fresh deionized (DI) water to remove PVA. Centrifugation was repeated. The supernatant was again removed and the particles resuspended with fresh DI water. The suspension was then frozen for approximately 45 min at -80C. Frozen particle suspension was lyophilized overnight.

3.2.6 Peptide Detection: Fluorescamine Assay Standard Curve

Ac-SDKP was diluted with PBS to the following concentrations starting with a 5 mg/ml stock solution: 100, 70, 50, 30, 10, 1, and 0 ug/ml. Each concentration of peptide (150 ul) was added to a black 96 well fluorescent microplate in triplicate. At the start of the assay, 50 ul of fluorescamine solution (3 mg/ml in acetone) was added to each well using a multichannel pipettor and measures were taken to protect the fluorescamine from light. The microplate was shaken by the plate reader for 45 sec. Fluorescamine reacts with primary amines (e.g. lysine on Ac-SDKP) and resultant product emits a detectable fluorescent signal at 460 nm when excited at 400 nm. Resultant fluorescence values were recorded.

3.2.7 Liquid-Liquid extraction technique verification

A specified amount of 1000 ug/ml (40, 20, 5, and 0.5 ul) of Ac-SDKP in PBS was added to 200 ul of chloroform in a 1.5 ml Eppendorf tube. The mixture was then vortexed rigorously for 30 sec. PBS (500 ul) was added to the Ac-SDKP/chloroform mixture. The mixture was again vortexed for 30 sec. In addition the mixture was further agitated by pipetting the aqueous phase through the organic phase and subsequently the organic phase through the aqueous phase. The mixture was then allowed to phase separate. The aqueous phase (470 ul) was removed from the mixture. Then 150 ul of the aqueous phase was place in a black 96 well fluorescence microplate in triplicate including 3 wells of a PBS blank. Ac-SDKP was detected and quantified per the fluorescamine assay protocol.

3.2.8 Ac-SDKP Particle Load Determination Technique Validation

Four different techniques were tested to ensure complete peptide release from particles and extraction from the organic phase. Particles used were from the same synthesis batch.

3.2.8.1 Method 1: rigorous agitation, emulsion droplets present

Approximately 1 mg of Ac-SDKP loaded particles was dissolved in 200 ul of chloroform in a 1.5 ml Eppendorf tube. The mixture was vortexed rigorously for 20 sec and 500 ul of PBS was then added to the mixture. Again the mixture was vortexed rigorously for and additional 10 min resulting in an emulsion. The emulsion was then phase separated partially, with emulsion droplets still visible. The aqueous phase (470 ul) was carefully removed and transferred to a second Eppendorf tube. Then 150 ul of the aqueous phase was placed in a black 96 well fluorescence microplate in triplicate including 3 wells of a PBS blank. Ac-SDKP was detected and quantified per the fluorescamine assay protocol.

3.2.8.2 Method 2: gentle agitation, emulsion droplets absent

Approximately 1 mg of Ac-SDKP loaded particles was dissolved in 200 ul of chloroform in a 1.5 ml Eppendorf tube. The mixture was vortexed rigorously for 20 sec and 500 ul of PBS was then added to the mixture. Then the mixture was vortexed gently for 10 sec and the tube inverted several times. The mixture was allowed to phase separate completely (i.e. no emulsion droplets present). Further agitation was achieved by pipetting the aqueous phase through the organic phase and subsequently the organic phase through the aqueous phase. The aqueous phase (470 ul) was carefully removed and transferred to a second Eppendorf tube. Then 150 ul of the aqueous phase was

place in a black 96 well fluorescence microplate in triplicate including 3 wells of a PBS blank. Ac-SDKP was detected and quantified per the fluorescamine assay protocol.

3.2.8.3 Method 3: rigorous agitation, emulsion droplets absent

Approximately 1 mg of Ac-SDKP loaded particles was dissolved in 200 ul of chloroform in a 1.5 ml Eppendorf tube. The mixture was vortexed rigorously for 20 sec and 500 ul of PBS was then added to the mixture. Again the mixture was vortexed rigorously for and additional 10 min resulting in an emulsion. The emulsion was then phase separated completely by centrifugation and pipetting. The mixture was centrifuged at 5000 rpm for 2 min and/or pipetted repeatedly until there was distinctive separation between the organic and aqueous phases. The aqueous phase (470 ul) was carefully removed and transferred to a second Eppendorf tube. Then 150 ul of the aqueous phase was placed in a black 96 well fluorescence microplate in triplicate including 3 wells of a PBS blank. Ac-SDKP was detected and quantified per the fluorescamine assay protocol.

3.2.8.4 Method 4: gently agitation, emulsion droplets present

Approximately 1 mg of Ac-SDKP loaded particles was dissolved in 200 ul of chloroform in a 1.5 ml Eppendorf tube. The mixture was vortexed rigorously for 20 sec and 500 ul of PBS was then added to the mixture. Then the mixture was vortexed gently for 10 sec and the tube inverted several times. The mixture was allowed to phase separate partially (i.e. some emulsion droplets present). The aqueous phase (470 ul) was carefully removed and transferred to a second Eppendorf tube. Then 150 ul of the aqueous phase was placed in a black 96 well fluorescence microplate in triplicate including 3 wells of a PBS blank. Ac-SDKP was detected and quantified per the fluorescamine assay protocol.

3.2.9 Ac-SDKP Particle Load Determination

Based on results from Particle Load Determination Technique Validation, method 3 was chosen as the standard load determination technique. This technique includes rigorous agitation and complete resolution of formed emulsion.

3.2.10 Peptide Release From Particles

Peptide release from particles exposed to a neutral pH was determined at a single time point. A time course of peptide release was not determined due to the insensitivity of the peptide detection assay. Approximately 2 mg of Ac-SDKP loaded particle was added to 1 ml PBS (pH 7.3). The particle suspension was incubated at 37 C and simultaneously agitated horizontally at 80 rpm. After 76 hrs, a 0.8 ml aliquot was removed and centrifuged at 14,000 rpm for 15 min. Ac-SDKP supernatant content was quantified using the fluorescamine assay.

3.2.11 Dynamic Light Scattering (DLS) Analysis

Dynamic light scattering is a technique that detects laser light scattering due to interference by small particles. The pattern of light scatter can be correlated to particle size distributions. During the particle synthesis process after solvent removal, but before particle washing an aliquot of particle suspension was reserved for DLS analysis. The particle suspension (1 ml) was placed in a clear plastic cuvett and diluted with DI water up to full cuvette capacity. Readings were taken over 1 min at 25 C to determine the particle effective diameter and particle size distributions.

3.2.12 Scanning Electron Microscopy (SEM)

Using a Hitachi S-800 SEM, high-resolution images were obtained of the lyophilized particles. Samples were prepared by affixing double-sided carbon tape to 12

mm pin type SEM mounts. Small amounts of particles were then spread across the topside of the carbon tape. Adhered particles were gold coated using a gold sputterer and imaged to visualize particle morphology.

3.2.13 Ac-SDKP Loaded Particle Bioactivity Assay

Ac-SDKP inhibition of TGF-ß induced FN expression was used as an assessment of peptide bioactivity (Gua 2004). RLSD primary fibroblasts were seeded at a density of 100,000 cells/well in a 12 well plate. Then the cells were allowed to recover and grow for 48 hrs in normal growth conditions (DMEM with 10% FBS, 1% penicillin/streptomycin). Next, we induced a state of cellular quiescence by placing cells in serum free DMEM media. After 24 hrs, cells were stimulated for 8 hrs according to the following treatments groups: 1) TGF-ß, 2) negative control (no treatment), 3) empty PK3 particles, 4) TGF-ß with empty PK3 particles, 5) free Ac-SDKP, 6) loaded Ac-SDKP particles, 7) pre-extracted Ac-SDKP from loaded PK3 particles. TGF-ß was administered at a final concentration of 5 ng/ml, free and extracted Ac-SDKP at 100 nM, and particles at 55 ug/ml. After treatment, RNA was isolated using the RNeasy Mini Kit (Qiagen) per manufacturers' instructions. Isolated RNA was quantified and assessed for purity by their 260:280 and 230:280 absorbance ratios. After which, quantitative real time polymerase chain reaction (qPCR) was performed to detect alterations of TGF-ß induced fibronectin expression. We used the Applied Biosystems Power SYBR Green I one-step RNA to Ct qPCR kit, which allows for cDNA synthesis and amplification in the same reaction vessel. Primer concentrations were 200 nM for both forward (5'-GTGGCTGCCTTCAACTTCTC-3') and reverse (5'-GTGGGTTGCAAACCTTCAAT-3') fibronectin primers (Yoshida et al. 2002) and 400 nM for both forward and reverse of ß-actin primers (Occam Biolabs). Forty ng of RNA template was used for each 20 ul reaction. Real time fluorescence was detected by the Applied Biosystems ABI 7700

Sequence Detector. Using RNA as a template, reverse transcription providing cDNA synthesis occurred at 48 C for 30 min. Then DNA polymerase was activated at 95 C for ten min. DNA amplification occurred during 40 thermocycles at 95 C for 15 sec followed by 60 C for 1 min. A melt curve was obtained for each reaction after each qPCR run to ensure single product formation.

3.3 Results

3.3.1 Ac-SDKP Loaded PK3 Particle Optimization

Various Ac-SDKP encapsulated PK3 particle synthesis techniques were investigated and optimized according primarily to Ac-SDKP load followed by particle size and polydispersity as summarized in Table 4. The w/o/w techniques designated as the "A series" evaluated the effect of the emulsion apparatus on particle analysis parameters. Upon initial assessment, the use of a sonicator and homogenizer for the primary and secondary emulsions respectively, yielded the highest Ac-SDKP loading at 3.59%. However, the loading efficiency could not be replicated in successive trials. Considering particle size, trials utilizing a votexer as the secondary emulsion device resulted in particles unsuitable for aerosolization with effective diameters ranging from 22- 42 um. The influence of the outer aqueous phase pH (i.e. the pH of the secondary emulgent solution), denoted as the "B series," resulted in a 6 fold increase in peptide loading at acidic pHs as compared to neutral. However, particle preparations at 5.3 and 1.6 outer aqueous phase pH, displayed elevated, undesirable effective diameters of 27 and 41 um respectively. We also examined the effect of the initial drug to polymer formulation on final Ac-SDKP load in the "C series." Results indicated that a preliminary 15% peptide to PK3 ratio was optimal, producing Ac-SDKP particle loads 0.1% above the standard initial 10% peptide to polymer ratio of the basic particle synthesis technique.

Given poor loading efficiencies and particle sizing from previous experimental perturbations, we further modified the particle synthesis technique despite trends of slight improvement. To address the aerodynamic particle criterion, we performed a synthesis procedure ensuring fabrication of porous particles. Particle porosity widens the size constraint necessary to maintain aerodynamic properties. By dissolving the PK3 polymer in a mixture of two organic solvents (hexane and DCM) with distinct vapor pressures, pores were formed during the solvent evaporation process. Following the secondary emulsion, we first evaporated DCM and the microspheres hardened leaving some hexane entrapped within the particles. Subsequently, at a higher temperature and pressure, hexane vaporized and in the process created pores upon release from the particles. Although, the particle size and morphology were consistent with the aerosolization criterion, with a diameter of 8 um, the Ac-SDKP loading remained low (0.25%).

In general the diminished Ac-SDKP loading may be attributed to loss during the final particle washing steps to remove the emulgent, PVA. Therefore, a 50% and 90% ethanol wash was performed. We attempted to interfere with Ac-SDKP loss to the aqueous wash due to the peptide's decreased solubility in ethanol. The resultant particle load of 0.29% suggested that a 90% ethanol wash positively affected peptide loading, but particle size was not conducive for aerosolization due to the particle aggregation observed (Figure 3). A final variation on the w/o/w double emulsion was investigated. We performed a cryo w/o/w technique, which is essentially invariable to the basic w/o/w emulsion, but preceding the secondary emulsion we snap froze the primary emulsion. This was an effort to hinder peptide release into the outer aqueous phase of the secondary emulsion and promote drug entrapment due to the peptide's frozen state. Evaluated Ac-SDKP particle loading and size achieved a similar value obtained by the 90% ethanol wash of 0.28% and 17 um.

Lastly, we examined a solid in oil in water emulsion method. This procedure was similar to previous w/o/w emulsion, but disperses solid peptide within the organic phase during the primary emulsion. Upon commencement of the secondary emulsion with the addition of an emulgent solution followed by agitation, for peptide loss to occur, it must first dissolve into the aqueous phase. This lengthens the duration the peptide remains emulsified in the organic phase and the probability that a microsphere will entrap the peptide. The data demonstrates this method's superiority for both maximizing Ac-SDKP loading while maintaining low particle sizes. Among independent replicate synthesis trials, peptide loading ranged from 0.48% to 1.93%, while particle sizes spanned 2.7 -5.5 um across trials. The average polydispersity measurement was 0.293, which indicates a relatively narrow distribution of particle sizes. Narrow size distribution should promote uniform peptide release from particles upon hydrolysis. In an attempt to further increase Ac-SDKP loading both the cryo w/o/w and s/o/w methods were performed with 90% ethanol washes. Consequently, peptide loading substantially decreased in both cases.

Table 4. Characterization of SDKP Loaded PK3 Microparticles. Detailed descriptions of protocols for each particle synthesis trial and SDKP load determination are given in the methods section. A series: Emulsion device modified; A1: 1-sonicator, 2-homogenizer; A2: 1-homgenizer, 2-vortex; A3: 1-sonicator, 2-vortex. B series: Outer aqueous phase pH modified; B1, 6.8; B2, 11.5; B3, 5.3; B4, 1.6. C series: Drug to polymer ratio modified; C1: 5%; C2 15%. Etoh wash: particles washed with ethanol at concentration indicated to remove 5% PVA after solvent evaporation. Effective diameter and polydispersity were determined by DLS. All loading values are adjusted for background levels determined from empty polyketals. *Basic synthesis technique. Standard deviations reported for Ac-SDKP load determined more than once for the same synthesis batch.

Trial	Ac-SDKP Loading (w/w)	Effective Diameter (um)	Polydispersity
*A1 replicate 1	3.59%	11.3	0.219
*A1 replicate 2	-0.06% ±0.01	6.0	0.243
*A1 replicate 3	-0.02% ±0.00	24.5	0.640
A2	1.50%	22.2	0.302
A3	0.13% ±0.11	41.9	0.487
*B1	0.04% ±0.01	14.6	0.201
B2	0.02%	33.4	0.475
B3	0.25% ±0.03	26.7	0.366
B4	0.24%	40.6	0.524
C1	0.05% ±0.04	9.0	0.137
C2	0.14% ±0.08	10.8	0.256
Porous	0.25% ±0.09	8.6	0.118
50% etoh wash	-0.01%	15.7	0.212
90% etoh wash	0.29%	20.7	0.283
Cryo w/o/w	0.28% ±0.06	17.8	0.646
S/O/W replicate 1	***0.48% ±0.36***	***5.5***	***0.177***
S/O/W replicate 2	***1.93% ±0.24***	***2.7***	***0.388***
S/O/W replicate 3	***1.20% ±0.61***	***4.6***	***0.153***
Cryo w/o/w with 90% etoh wash	0.07% ±0.11	19.9	0.285
S/O/W with 90% etoh wash	0.21% ±0.07	6.1	0.174

3.3.2 Ac-SDKP Peptide Detection: Fluorescamine Standard Curve

An Ac-SDKP standard curve was generated using a fluorescence assay utilizing fluorescamine. Fluorescamine reacts with primary amines and consequently emits a detectable fluorescent signal at 460 nm when excited at 400 nm. Ac-SDKP has one free amine located on lysine and was quantified with acceptable precision and accuracy utilizing this assay. Three independent curves were created incorporating Ac-SDKP concentrations up to 100 ug/ml. After linear regression analysis, slopes obtained were 11.254, 11.543, and 10.572 with respective R^2 values of 0.9947, 0.9952, and 0.9976 (Figure 1). For Ac-SDKP quantification in the peptide particle load determination, the average slope (11.123 $\pm$0.50) was used.

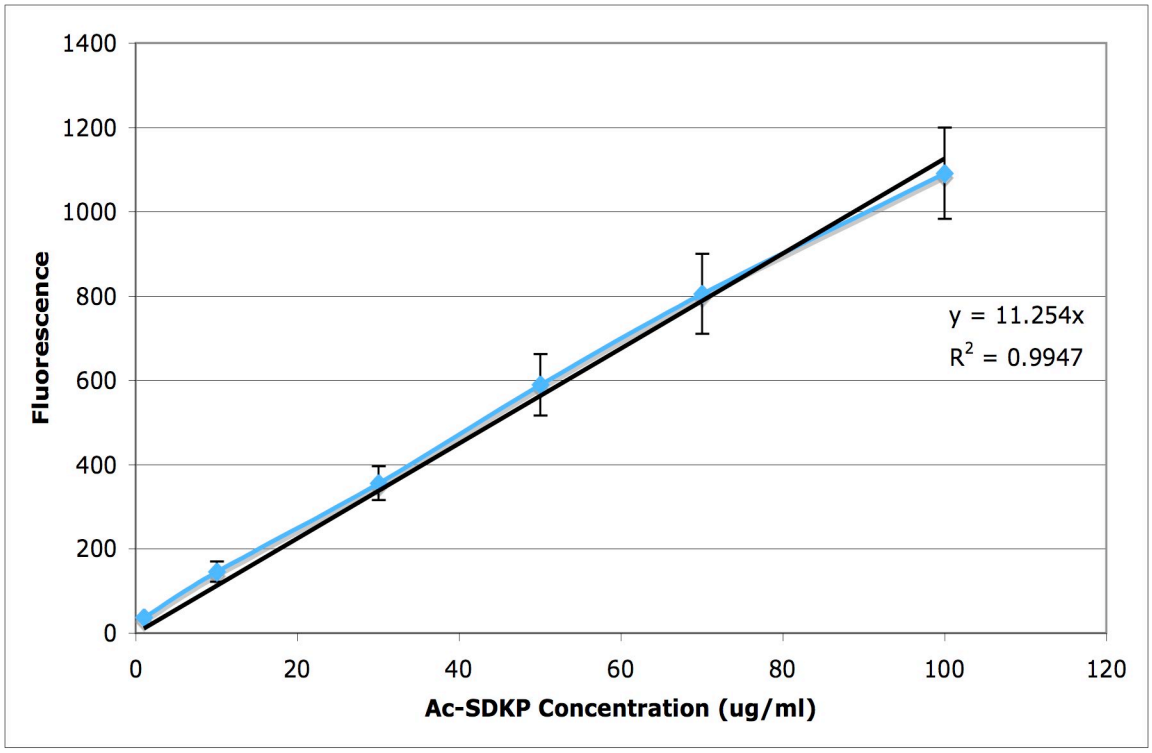

Figure 1. Ac-SDKP Standard Curve. The standard curve was generated using the fluorescamine assay. On the basis of this curve, concentrations of Ac-SDKP extracted from loaded PK3 particles were quantified. The above curve is representative of three independent curves generated. The remaining independent curves resulted in slopes of 11.543 and 10.572 with R^2 values of 0.9952 and 0.9976 respectively. The average slope of all three independent trials (11.123 $\pm$0.50) was used for Ac-SDKP quantification.

3.3.3 Liquid-Liquid Extraction Technique Validation

To ensure Ac-SDKP is not appreciably soluble in the organic phase (chloroform) used during peptide extraction from PK3 for particle load determinations, we validated the extraction technique. Rigorously mixing known concentrations of Ac-SDKP in chloroform and then extracting the peptide with the addition of an aqueous solution allowed a comparison between theoretical Ac-SDKP amounts introduced and the actual Ac-SDKP concentrations calculated by use of the fluorescamine assay. Concentrations of Ac-SDKP tested ranged from 1 to 80 ug/ml. In the lower concentration range, error remained within less than 10%. With high concentrations error was miniscule and was within 1% (Table 5).

Table 5. Liquid-Liquid Extraction Technique Validation. A known concentration and amount of Ac-SDKP was subjected to the established extraction technique of the peptide from polyketals particles. Various amounts of free Ac-SDKP were immersed and mixed in an organic solvent and subsequently extracted with the addition of an aqueous phase. The extraction protocol followed the previously detailed SDKP Load Determination as found in the methods section absent the PK3 particles.

Ac-SDKP Concentrations		
Theoretical (ug/ml)	**Actual (ug/ml)**	**Percent Error**
40	39.60	0.98
80	80.79	0.99
10	9.03	9.60
1	0.93	6.76

3.3.4 Ac-SDKP Particle Load Determination Technique Validation

To promote complete release of Ac-SDKP from synthesized particles, the rigor and procedure of extraction were investigated. This ensures accurate determination of the Ac-SDKP loading in PK3 particles, so that optimal synthesis conditions can be

identified. We evaluated four distinct methods. Method one involved rigorous agitation, allowing an emulsion to form. We partially resolved the emulsion and then removed the aqueous phase for quantification of Ac-SDKP by the fluorescamine assay. In method two, readings were obtained after gentle agitation with no emulsion formation. Method three again involved rigorous agitation, but included complete resolution of the formed emulsion by centrifugation. Lastly, in method four after gentle agitation and the presence of emulsion droplets, Ac-SDKP was quantified. Using particles obtained from the same synthesis batch, method three yielded the most detectable peptide at 0.24% loading (Table 6). This 2.6 fold increase above method 1, suggests that for maximal peptide extraction from PK3 and the organic phase, rigorous agitation to the point of emulsion formation followed by complete resolution is needed.

Table 6. Ac-SDKP Particle Load Determination Technique Validation. Varying methods of a liquid-liquid extraction technique were performed to promote maximal Ac-SDKP peptide release from the loaded PK3 particles and the organic phase. In depth descriptions of techniques are provided in the methods section. Method 1: rigorous agitation, emulsion droplets present. Method 2: gentle agitation, emulsion droplets absent. Method 3: rigorous agitation, emulsion droplets absent. Method 4: gentle agitation, emulsion droplets present.

Method	SDKP Loading (w/w)
1	0.094%
2	0.088%
3	0.24%
4	0.16%

3.3.5 Peptide Release From Particles

By incubating and agitating a 2 mg/ml Ac-SDKP loaded particle suspension, we obtained a measure of peptide release from PK3 particles. After 76 hrs of incubation at 37 C, the suspension supernatant was tested for Ac-SDKP content and compared to peptide loading as determined by liquid-liquid extraction. We found that by 76 hrs in

PBS (pH7.3), 92% of encapsulated peptide was released. This indicates rapid particle hydrolysis. *In vivo*, this property will promote effective therapeutic dissemination as well as timely clearance of degraded byproducts.

3.3.6 Particle Morphology Characterization

After determination of Ac-SDKP particle loading from various synthesis trials, Scanning Electron Micrographs were captured for methods yielding increased peptide loading. Visualization enables assessment of particle integrity and the uniformity of particle morphology. For the "A series," we verified particle formation due to the stringency disparities among emulsion devices. A1, which utilized a sonicator and homogenizer for the primary and secondary emulsions respectively yielded rough, but consistent particles. The trial utilizing a sonicator for the first emulsion and vortex for the second (A3), demonstrates successful particle formation, but with a significant population of large particles. However, for A2 (homogenizer- first emulsion; vortex- second emulsion), despite high Ac-SDKP loading at 1.5%, inconsistent and low particle formation was observed. From this, we can ascertain that a sonicator is necessary for the first emulsion step in order for particle synthesis to be successful (Figure 2).

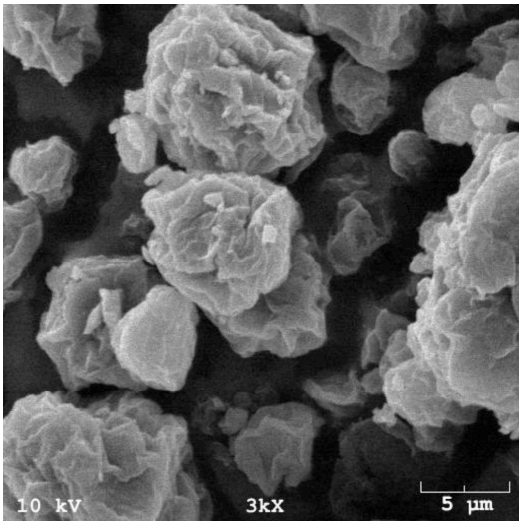

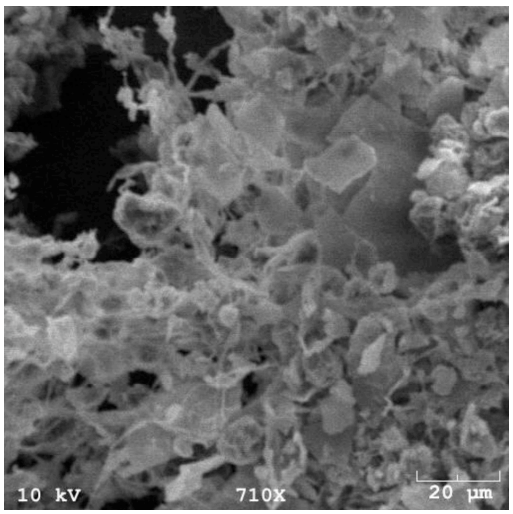

A1 **A2**

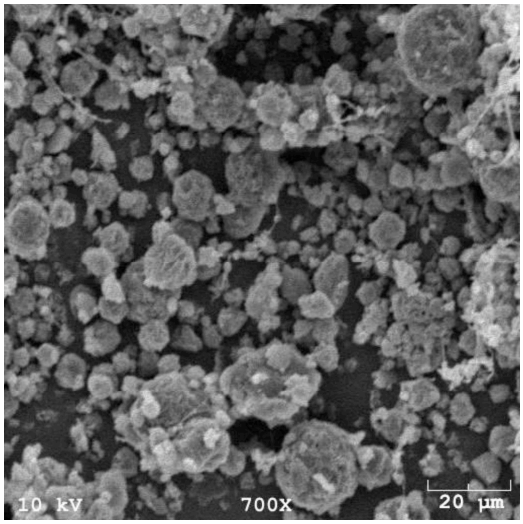

A3

Figure 2. SEM of A Series Particles. Scanning Electron Micrographs taken of A series particle synthesis techniques. The A series varied the emulsion devices used for both the primary and secondary emulsions. Emulsion device modified; A1: 1-sonicator, 2-homogenizer; A2: 1-homgenizer, 2-vortex; A3: 1-sonicator, 2-vortex.

The three s/o/w replicates yielding a high Ac-SDKP load were also imaged. Micrographs illustrate successful, consistent particle synthesis and relatively low polydispersity. However, surface morphology does appear variable among the trials. This is due to the use of different PK3 polymer batches, which inevitably possess variance. Other results do not indicate any further affect on particles due to PK3 inconsistency. In addition, the s/o/w trial with a 90% ethanol wash was visualized. Images suggest that ethanol is incompatible with PK3 and effectively damages particle formation, which can be observed in Figure 3.

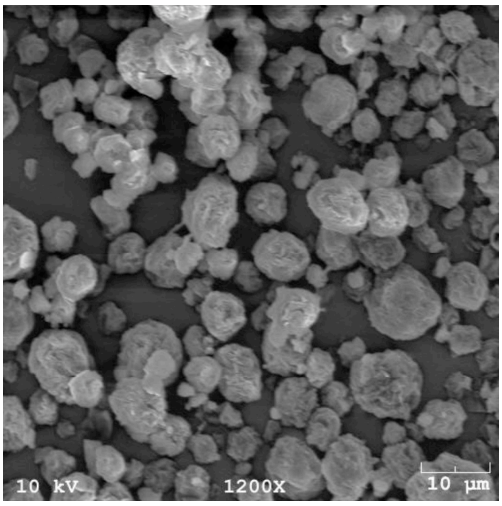

Replicate 1

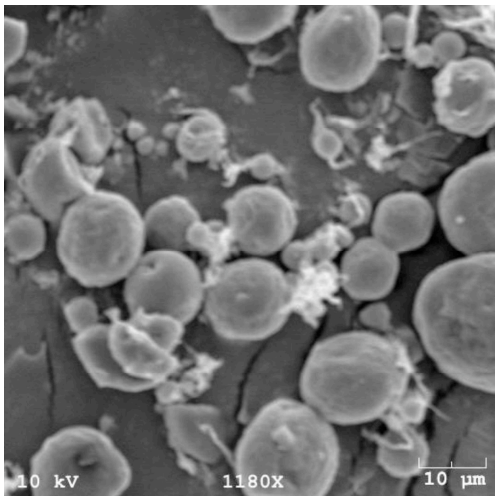

Replicate 2

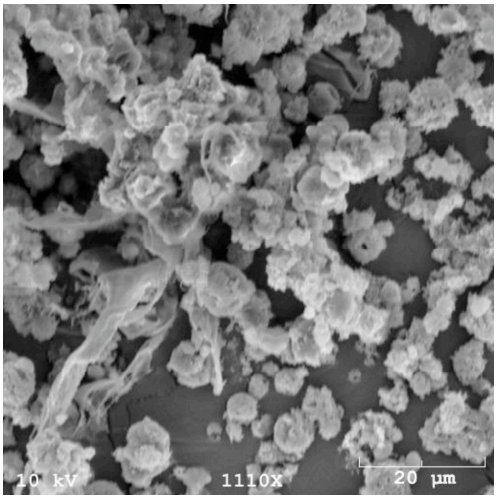

Replicate with 90% ethanol wash

Figure 3. SEM of S/O/W Particles: Replicate Trials. Scanning Electron Micrographs taken of the solid in oil in water emulsion technique particles synthesized. Three independent replicate trials were performed and imaged. A detailed description of the synthesis technique can be found in the methods section.

3.3.7 Ac-SDKP Biochemical Activity After Release From Particles

Following Ac-SDKP encapsulation within PK3 microparticles, we evaluated the preservation of the entrapped peptide's bioactivity. This determination is essential to verify maintenance of Ac-SDKP's anti-fibrotic properties. Previous work indicates that Ac-SDKP effectively reduces TGF-ß induced fibronectin mRNA expression (Guo et al. 2004, Hocevar et al.1999). By stimulating primary rat fibroblasts with TGF-ß and simultaneously subjecting the cells to various particle and Ac-SDKP treatments, we elucidated particle processing effects on Ac-SDKP bioactivity.

Fibronectin (FN) mRNA levels were quantified via qPCR. To assess relative changes in FN expression due to experimental treatments, we utilized the Gene Expression's C_T Difference formula (Figure 4). The formula compares a gene of interest relative to a housekeeping gene in a particular treatment sample to a reference sample usually designated as the experimental control. This analysis technique accounts for variant PCR efficiencies and permits relative quantification of a gene of interest without knowledge of an initial gene copy number or standard curve (Schefe et al. 2006). For this study, our reference sample was our positive control of TGF-ß cellular stimulation. In addition, our housekeeping gene, which should be unaffected by varying cellular treatments was ß-actin.

$$rER = \frac{R_{norm}(SOI)}{R_{norm}(ref)} = \frac{(1+E(FN))^{-\Delta C_T(FN)}}{(1+E(\beta actin))^{-\Delta C_T(\beta actin)}}$$

Figure 4. Gene Expression's C_T Difference Formula: Relative Expression Ratios (rER). This formula was used to determine the relative expression of FN among experimental treatment groups assessing Ac-SDKP bioactivity. R_{norm}, normalized fluorescence; SOI, sample of interest; ref, reference sample; E(FN), efficiency of FN; E(ß-actin), efficiency of ß-actin;
$\Delta C_T(FN) = C_T(FN, SOI) - C_T(FN, ref)$; $\Delta C_T(ß\ actin) = C_T(ß\ actin, SOI) - C_T(ß\ actin, ref)$.

All cellular treatments included simultaneous stimulation of FN expression by TGF-ß. Results reveal, consistent with current literature, cells exposed to free Ac-SDKP substantially down regulate FN mRNA expression. Resultant mRNA expression is 70% below levels obtained from cells solely stimulated by TGF-ß (Guo et al. 2004, Hocevar et al.1999). For empty PK3 particle treatments, particles were administered at concentrations as if loaded with 1% (w/w) Ac-SDKP that correlated with free Ac-SDKP dosing. We further increased empty particle concentrations 10 fold from those correlating to free SDKP administration to ensure evident responses. The empty PK3 particle cellular treatment demonstrates an insignificant affect on FN expression. In addition, cells were exposed to 1.2% Ac-SDKP loaded particles synthesized by the s/o/w emulsion technique at the same concentration as empty particles. Results illustrate a FN relative expression ratio (rER) as compared to the positive control (TGF-ß only stimulation) of 1.65. Concurrently, pre extracted Ac-SDKP from the same particle batch and similar dosing to free SDKP also induced an up regulation of Fn expression with a relative expression ratio of 1.45. Upregulation of FN expression due to exposure to previously processed Ac-SDKP indicates severe loss of bioactivity. Peptide processing appears to have an adverse effect on FN expression leading to overproduction above levels induced by TGF-ß alone (Figure 5).

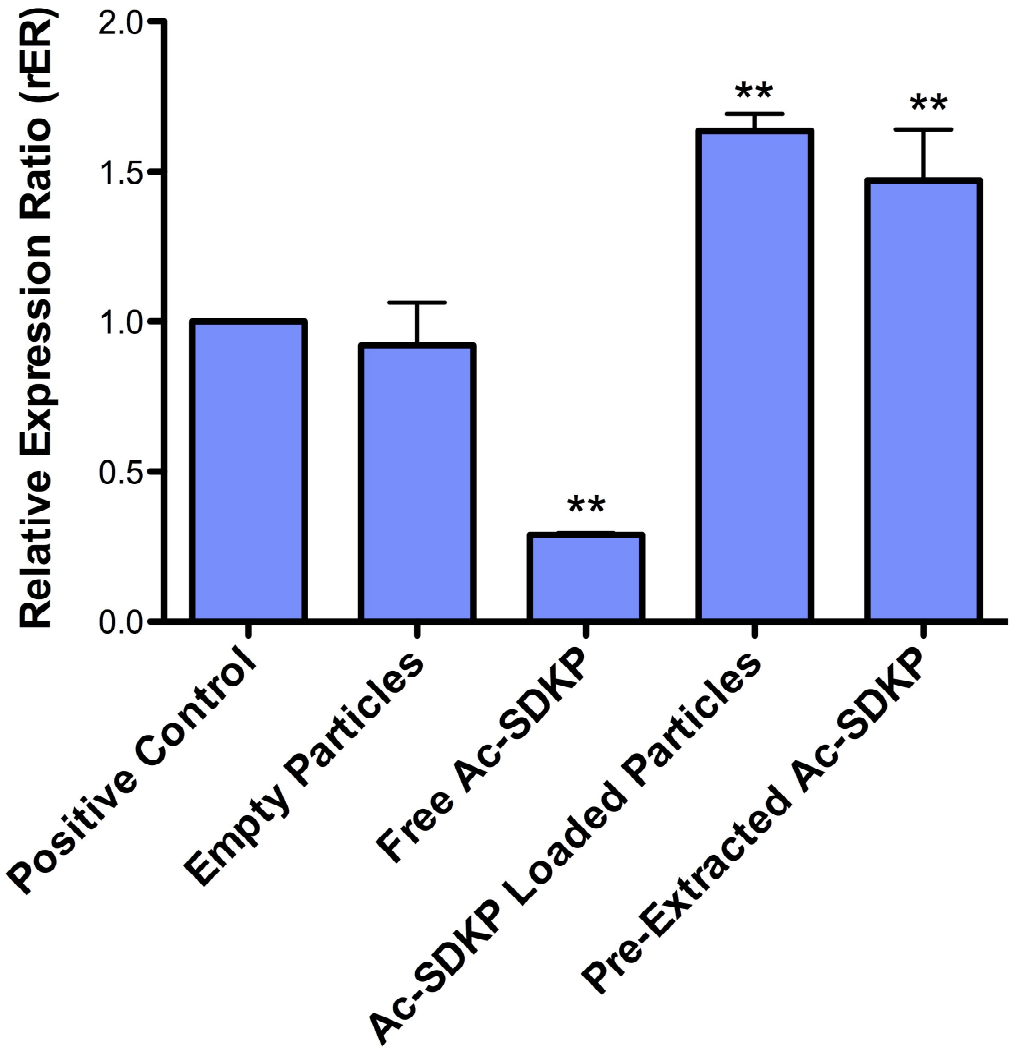

Figure 5. Relative Fibronectin mRNA Expression Ratio Following Ac-SDKP Treatment. Cells were simultaneously exposed to TGF-ß with indicated treatments for 8 hours and relative Fn expression ratios were determined by qPCR. Treatments included TGF-ß alone, empty PK3 particles, free Ac-SDKP, Ac-SDKP loaded particles, and pre-extracted Ac-SDKP from loaded particles. rER's were determined using the Gene Expression's C_T Difference Formula. **$p<0.01$ as compared to positive control.

3.4 Discussion

Use of polyketal microparticles as a drug delivery vehicle can expand non-invasive treatment possibilities specified for pulmonary applications. In this study, we proposed we could optimally load the model therapeutic, Ac-SDKP, into polyketal microparticles possessing aerodynamic properties conducive for aerosolization. We identified key parameters such as the emulsion device, pH, drug/polymer formulation, and type of emulsion in the particle synthesis process that have influence on peptide loading and particle size distribution. Systematic alterations of these parameters and characterization of resultant particles allowed us to maximize Ac-SDKP loading while adhering to aerodynamic size constraints.

Through evaluation of Ac-SDKP loading we found a probe sonicator is the only apparatus capable of effectively emulsifying the primary emulsion of the particle synthesis process. Use of a homogenizer or vortex does not supply the agitation necessary to properly disperse the peptide throughout the inner organic phase of the double emulsion. This failure is likely due to peptide emulsion droplets being too large and thus thwarting the possibility of the polyketal to form a microsphere surrounding the peptide. The pH of the outer aqueous phase of the double emulsion did have a slight positive affect on Ac-SDKP loading, but had more influential effect on particle size. At acidic pHs, particle size ranged from approximately 20-40 um, which is incompatible with aerosolization. This trend is consistent with previous studies (Peltonen 2004). The initial peptide/polymer formulation appeared to have minor affects on final Ac-SDKP loading. We discovered that an initial 15% drug to polymer ratio slightly increases final loading. With more peptide available for encapsulation during the processing, the probability of entrapment is likely increased. However, the aforementioned particle synthesis parameters do not have a robust effect on final Ac-SDKP loading. Therefore, we further modified the basic w/o/w emulsion technique.

We performed a synthesis technique specified for the creation of porous particles since previous trials resulted in non-porous particles too large for aerosolization. During particle processing, the polyketal polymer was dissolved in a mixture of two organic solvents with distinct boiling points. At the solvent evaporation step, the less volatile solvent remained trapped within hardened, formed microparticles. Then upon evaporation of the entrapped solvent, pores were formed as the solvent released from the particles. This procedure was successful in creating aerodynamically suitable particles, but lacked sufficient Ac-SDKP loading. In addition, a cryo w/o/w emulsion method was assessed. This method involved snap freezing the primary emulsion, so Ac-SDKP loss to the outer aqueous phase of the secondary emulsion was minimized. Again, this method displayed slight increases in Ac-SDKP loading but failed to maintain prescribed aerodynamic constraints. This was likely due to the inability of the homogenizer to completely unify the mixture due it being partially frozen leading to larger particles.

Lastly, a solid in water in oil emulsion was performed in attempt to attain particle design specifications. The procedure was comparable to the basic w/o/w technique previously used, except we emulsified solid peptide within the inner organic phase of the primary emulsion. This technique significantly increased peptide loading and produced particles within a range suitable for aerosolization. Peptide loss to the outer aqueous phase of the secondary emulsion was likely minimized due to the lengthen duration the peptide remained in the organic phase. The peptide must first dissolve in the aqueous phase for loss to occur, which increases the probability polyketal polymer will encapsulate the peptide. Resultant Ac-SDKP loading ranged from 0.5%-1.9% (w/w) which should translate to clinical dosing requirements. Previous studies have shown a 1 mg/kg dose of Ac-SDKP was effective in asserting anti-fibrotic effects. Therefore 0.5% Ac-SDKP loading, if locally dispensed should be efficacious.

Once particles were produced at Ac-SDKP loading levels translatable to clinical dosing needs, the bioactivity of the released peptide was examined. From past studies, it is known that TGF-ß induced FN expression is effectively down regulated by the peptide Ac-SDKP (Guo et al. 2004, Hocevar et al.1999). By quantifying FN mRNA levels after *in vitro* stimulation of cells with TGF-ß followed by treatment with Ac-SDKP loaded microparticles, peptide bioactivity was assessed. Results indicated that Ac-SDKP extracted from previously synthesized particles as well as loaded particles unexpectedly upregulated FN mRNA expression in primary fibroblasts. In contrast, free Ac-SDKP inhibited FN expression and empty PK3 particles had no significant effect on FN expression. This suggests there are alterations to the peptide due to the particle synthesis process. Throughout the particle synthesis process the peptide is subjected to various treatments including exposure to organic solvents and intense mechanical manipulations that could have adverse effects on its bioactivity. Future studies will have to determine the stage in the particle synthesis process peptide alterations occur and how structurally the peptide is distorted. If this can be determined then it may be possible to restore Ac-SDKP bioactivity following release from loaded PK3 particles.

CHAPTER 4

BIOCOMPATIBILITY OF POLYKETAL MICROPARTICLES

4.1 Introduction

It is vital for pulmonary applications that delivered substances do not elicit a significant inflammatory response. As observed in many chronic lung disorders, inflammation is a salient feature and facilitates fibrotic events leading to lung function compromise. Therefore, an effective delivery vehicle should not exacerbate the already inflamed tissues and exhibit exceptional biocompatibility. To assess polyketal biocompatibility, responses to particle exposure were investigated both *in vivo* and *in vitro*. The *in vivo* assessment involved the intratracheal injection of empty particle suspensions (both PLGA and PK3) into murine models and subsequent analysis of bronchoalveolar lavage (BAL) fluid as well as histological examination. The BAL and the histological examination should reveal any increase in inflammatory and/or immune cells due to particle presence. Also, injection of PLGA particles will permit the demonstration of PK3 as a superior biocompatible biomaterial. The *in vitro* study, performed with the U937 monocytic cell line, aims to reveal any cell activation causing IL-1 expression due to exposure to the particles. Ideally, inflammatory responses as well as cytokine production should remain minimal or similar to basal levels despite the presence of the PK3 particles.

4.2 Methods

4.2.1 Materials

PK3 polymer (donated by the Murthy lab), Poly (dl- lactide/glycolide) 50:50 (Polysciences, Inc., Warrington, PA) U937 IL-1 (Interleukin-1) luciferase reporter construct cells (donated by the Roman lab), RPMI 1640 media (Mediatech, Herndon,

VA), Fetal Bovine Serum (Mediatech, Herndon, VA), Penicillin-Streptomycin (Mediatech, Herndon, VA), CellGro COMPLETE media (Mediatech, Herndon, VA), Lipopolysaccharide (Sigma, St. Louis, MO), Luciferase Detection kit (Promega, Madison, WI) C57 BL6 male mice (Jackson Labs, Campbell, CA) ketamine/xylazine, 10% buffered Formalin (VWR International, Suwanee, GA), Lueco Stat Kit (Fisher Scientific, Pittsburgh, PA), Hematoxylin and Eosin stain (Richard-Allan Scientific, Kalamazoo, MI), Paraffin (Surgipath Medical Industries, Richmond, IL).

4.2.2 Empty Particle Synthesis

Synthesis of empty particles was achieved by a double emulsion technique similar to previously described methods. Particle size and morphology were characterized by DLS and SEM respectively.

4.2.2.1 PK3 Particle Synthesis

PVA (1%, 500 ul) at pH 8.5 was added to an 8ml glass vial. In a separate 24 ml glass vial, 500 mg of PK3 was dissolved in 5 ml of dichloromethane (DCM) to also yield a 100 mg/ml solution. The PK3 in DCM solution was then added to the 1% PVA solution and emulsified with the homogenizer (level 5) for 1.5 min. Immediately, 20 ml of a 5% PVA buffered (pH 6.8) solution was added to this primary emulsion and homogenized (level 3) for 1.5 min yielding the secondary emulsion. The emulsion was added to a 500 ml round bottom flask and DCM is removed with the use of a Rotovap. The flask was rotated at speed 3 for the duration of the evaporation process, which included cycling the mixture between low and high pressures over the course of approximately 10-15 min. Contents of the 500 ml round bottom flask (particle suspension) were then dispensed into a 50 ml conical tube and diluted with deionized water to approximately 50 ml. A 1 ml aliquot of the particle suspension was reserved for dynamic light scattering analysis

to determine particle size distributions. The particle suspension was then centrifuged for 10 min at 7000xg. The supernatant was removed and particles resuspended by vortexing with 40 ml of fresh deionized (DI) to remove PVA. Centrifugation was repeated. The supernatant was again removed and the particles resuspended with fresh DI water. The suspension was frozen for approximately 45 min at -80 C. Frozen particle suspension was lyophilized overnight. This procedure was repeated to yield an approximate 1 g batch of empty particles.

4.2.2.2 PLGA Particle Synthesis

PVA (1%, 500 ul) at pH 8.5 was added to an 8ml glass vial. In a separate 24ml glass vial, 500 mg of PLGA was dissolved in 5ml of dichloromethane (DCM) to also yield a 100 mg/ml solution. The PLGA in DCM solution was added to the 1% PVA solution and emulsified with the homogenizer (level 5) for 1.5 min. Immediately, 20 ml of a 5% PVA buffered (pH 6.8) solution was added to this primary emulsion and homogenized (level 4) for 1.5 min yielding the secondary emulsion. The emulsion was added to a 500 ml round bottom flask and DCM is removed with the use of a Rotovap. The flask was rotated at speed 3 for the duration of the evaporation process, which included cycling the mixture between low and high pressures over the course of approximately 10-15 min. Contents of the 500 ml round bottom flask (particle suspension) were then dispensed into a 50 ml conical tube and diluted with deionized water to approximately 50 ml. A 1ml aliquot of the particle suspension was reserved for dynamic light scattering analysis to determine particle size distributions. The particle suspension was then centrifuged for 10 min at 7000xg. The supernatant was removed and particles resuspended by vortexing with 40 ml of fresh deionized (DI) water in order to wash and remove PVA. Centrifugation was repeated. The supernatant was again removed and the particles resuspended with fresh DI water. The suspension was then frozen for about 45 min at -

80 C. Frozen particle suspension was lyophilized overnight. This procedure was repeated to yield an approximate 1 g batch of empty particles.

4.2.3 *In Vitro* Cytokine Response to Particles

U937 cells (monocytic) transfected with an IL-1 luciferase reporter construct, were transitioned into CellGro COMPLETE serum free media from growth media (RPMI 1640) over two days. We seeded cells at a density of 500,000 cells/well (200 ul) in a 48 well plate and then allowed the cells to reach a state of quiescence in serum free media over 36 hrs. PLGA and PK3 particles were suspended at a concentration of 0.7 mg/ml in serum free media and LPS dissolved in media at a concentration of 3 ug/ml. Both particle suspensions (100 ul) as well as LPS (100 ul) were added to the cells in triplicate for two time points (24, 48 hrs). For a negative control, 100 ul of culture media was added in triplicate for 3 time points: 0, 24, 48 hrs. At specified time points, well contents were aspirated and placed in a 1.5 ml Eppendorf tube. The tubes were then centrifuged at 10,000 rpm for 10 min to pellet cells and particles. The supernatant was carefully removed and pellet stored in a clean eppendorf tube at -20 C for later analysis of luciferase activity.

We quantified luciferase activity using a luciferase activity assay by Promega. Cell pellets were lysed in luciferase assay lysis buffer (50 ul) and sonicated for 10 sec. Then 20 ul of each lysed sample was added to an opaque microplate. We added 50 ul of the luciferase substrate and read luminescence after 3 min. A total protein assay was also performed to account for minor variations among sample cell numbers. We added 10 ul of the lysed sample to a clear microplate and added 200 ul of 1:4 diluted Bio Rad dye reagent. Absorbance was read at 595 nm. Luminescence values were all normalized to the sample with the highest protein content.

4.2.4 Intratracheal Particle Injections (Murine Model)

Particles were injected intratracheally into C57 BL6 male mice (20-25g) to assess polyketal biocompatibility *in vivo*. All mice were anesthetized according to IUCUC standards by injection interperitoneally with 200 ul of ketamine/xylazine solution (approx. 80mg/kg ketamine + 10 mg/kg xylazine). Then a small incision was made at the throat to expose the trachea. Using a sterile syringe, the trachea was punctured and particle suspensions injected. Experimental groups included particle suspensions composed of 1.5 mg of PK3 (n=3) and 1.5 mg of PLGA (n=3) in 50 ul of sterilized PBS. In addition, control groups included bleomycin as a positive (n=2), PBS as a vehicle (n=2), and unadulterated mice as a negative (n=2). After injections, mice were sutured and left to recover. For the experimental and bleomycin groups, mice were sacrificed at days 1, 4, and 7. For the vehicle control, mice were sacrificed at day 5, and the unadulterated control group at day zero. Immediately following sacrifice by sufficient CO_2 (approx. 3 min) gas inhalation a bronchoalveolar lavage was performed and the lung harvested.

4.2.5 Bronchoalveolar Lavage (BAL)

Once the mice were euthanized by CO_2 gas, the throat was again cut to expose the trachea. A syringe with 1.5 ml of sterile PBS was dispensed into the trachea and subsequently filled all five lobes of the lung. After the syringe was completely plunged, the dispensed PBS was then recovered by suction of the syringe. Cells and fluid collected were place on ice in 1.5 ml Eppendorf tubes. Following centrifugation at 4000 rpm for 7 min, cell pellets were resuspended in 100 ul of PBS. BAL samples were prepared for staining and quantification by standard cytospin procedures. Using the Cytospin 2 (Shandon Inc.) cells were centrifuged onto slides at 1500 rpm for 7min. Resulting slides were fixed and stained using Lueco Stat Kit (Fisher Scientific).

4.2.6 Lung Harvesting and Histology Examination Preparation

Immediately following the BAL, lungs were harvested from at least one mouse from each time point and experimental/control group. Skin and various internal organs were resected systematically to harvest the lungs. The trachea was cannulated and left in tact upon removal of the lungs from the body. Using the cannula, the lungs were inflated with 10% buffered formalin and then stored in 15 ml of 10% buffered formalin until paraffin embedding. Lungs were embedded in paraffin and sectioned into 5 um slices. Slices were processed according to standard techniques and stained with hematoxylin and Eosin (H&E) on slides.

4.3 Results

4.3.1 Empty Particle Characterization

Empty PK3 and PLGA particles were evaluated by size and morphology. We aimed to produce particles that were consistent with loaded particles previously synthesized as well as with the prescribed size design criteria. PLGA and PK3 particles were synthesized in two batches. Both batches of each polymer were combined before intratracheal administration. Particles size and morphology are detailed in Table 7 and Figure 6 respectively.

Table 7. Summary of Particle Characterization For The Animal Study. Diameters and polydispersity measurements were obtained from the DLS instrument. Batches were combined prior to intratracheal injection into the murine model.

Particle Batch	Effective diameter (um)	Polydispersity
PK3 Batch 1	1.06	0.074
PK3 Batch 2	0.89	0.005
PLGA Batch 1	0.77	0.005
PLGA Batch 2	0.70	0.206

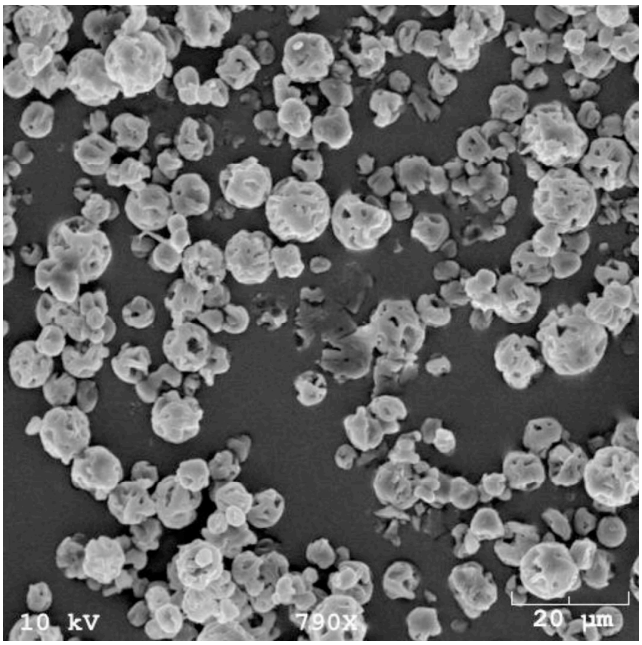

PK3

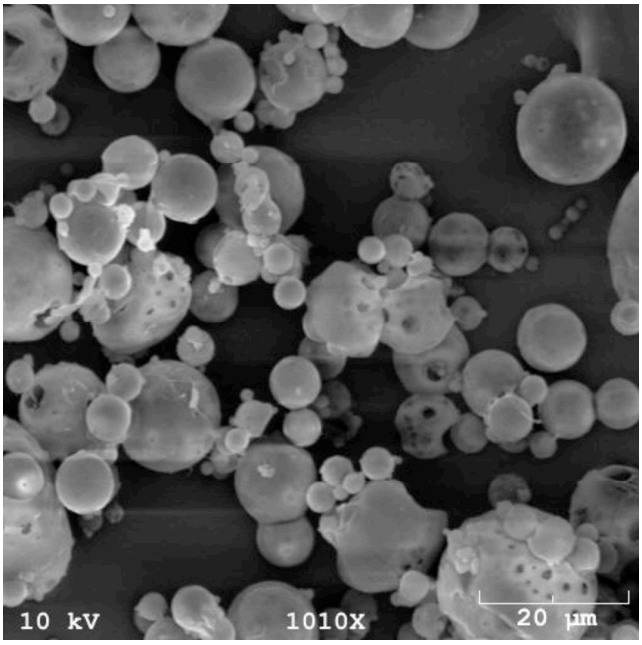

PLGA

Figure 6. SEM of Particles Used For Intratracheal Injections. Empty PLGA and PK3 particles were synthesized for use in intratracheal injections into a murine model. Particles were created in two separate batches that were combined prior to injections. Images are representative of the particles injected and are from one of the two batches prior to combining.

4.3.2 Bronchoalveolar Lavage Analysis

To determine pulmonary biocompatibility of polyketals, we intratracheally injected 1.5 mg of particles into a murine model. For comparison, the current commonly used biomaterial for drug delivery, PLGA, was also injected to demonstrate PK3's superiority in minimizing inflammation induction. The controls included injection of a known inflammation inducer, bleomycin, the vehicle, PBS (sacrificed at day 5), and an unadulterated control. Particle treatment as well as bleomycin groups were sacrificed at the 1, 4, and 7 day time points for BAL analysis and histological examination. After procuring BAL fluid and affixing collected cells to slides, we performed a cell count of major inflammatory/ immune cells. Results indicate the starkest contrast with macrophage counts among treatment groups (Figure 7). At day 1, the PK3 treatment group exhibits no statistical difference from unadulterated and vehicle controls; whereas, PLGA shows extreme significance from negative controls, suggesting a heighten inflammatory response. At day 4, both PK3 and PLGA particle groups demonstrate increased infiltration of macrophages. However, by day 7 for PK3 injections, macrophage levels abated, while PLGA induced macrophage counts continued to increase. Assessment of lymphocytosis revealed at day 4, PLGA may elicit a slight cell mediated immune response. In contrast, PK3 facilitated lymphocyte counts among all time points, remained similar to basal levels. Lastly, examination of BAL fluid neutrophil content displayed a slight increase at day 1 in PK3 induced neutrophil infiltration as compared to the unadulterated control group. However, for days 4 and 7, populations of neutrophils for both PK3 and PLGA groups, were not statistical variant from negative control groups (Figure 7).

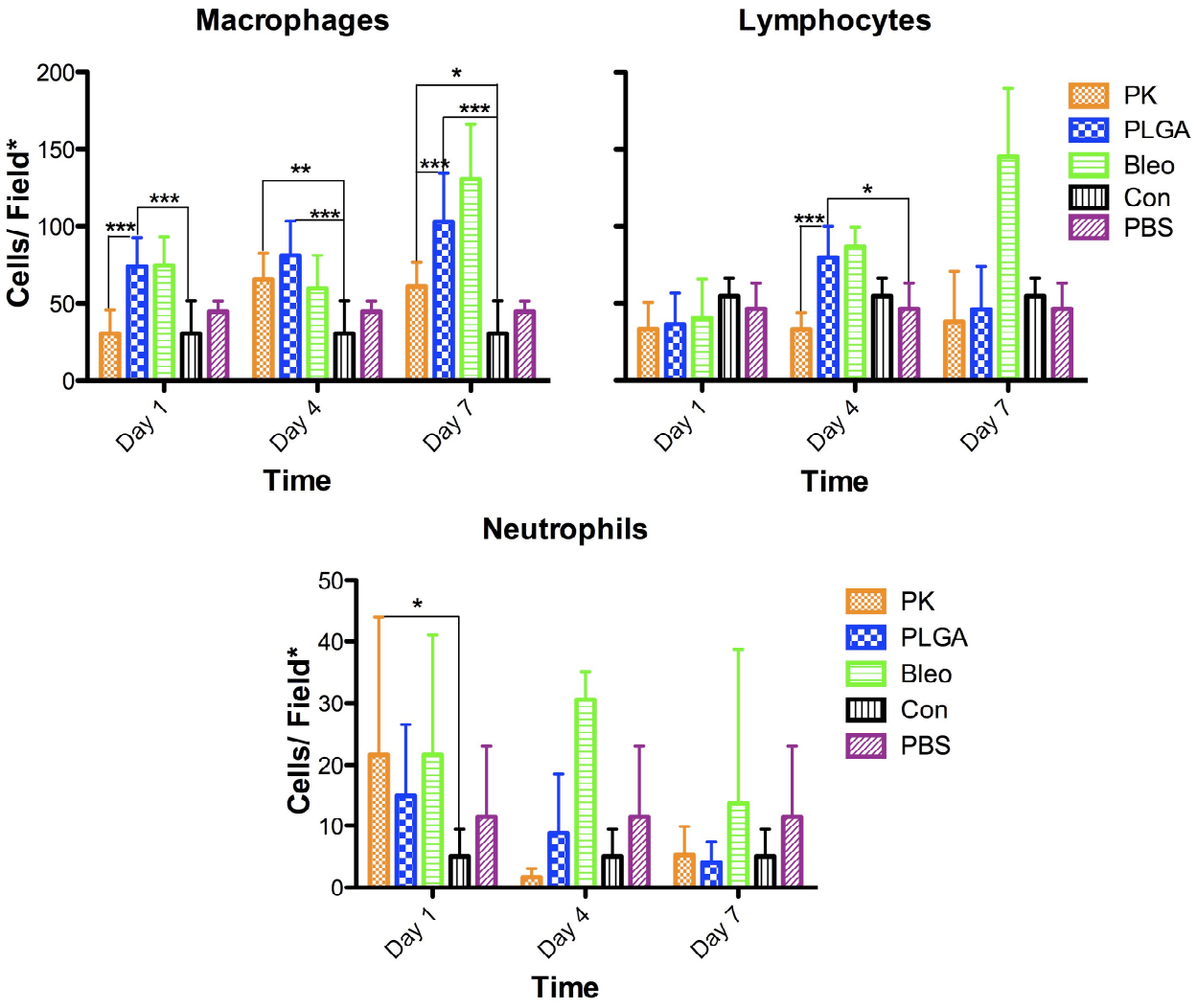

Figure 7. Bronchoalveolar Lavage Analysis After Intratracheal Particle Injections. PK (n=3) and PLGA (n=3) particles were injected and BAL fluid analyzed for inflammatory/immune cell content. Control groups included bleomycin (Bleo, positive, n=2), vehicle (PBS, negative, n=2), and unadulterated mice (Con, negative, n=2). *p<0.05, **p<0.01, ***p<0.001. *Field is approx 0.14mm^2.

4.3.3 Histological Assessment of Polyketal Effect

Following BAL fluid procurement, at least one lung from each time point and experimental group was extracted for histological examination. We assessed, qualitatively, stained lung slices based on inflammatory cell presence and lung structure. Slides were scored based on the following scale: 0, no inflammation; 1, some inflammation; 2, more inflammation; and 3, most inflammation. Results appear to corroborate BAL data in that PK3 particles do not induce significant inflammatory responses (Figure 8, 9). Scoring suggests PLGA is more inflammatory than PK3 with elevated scores at days 1 and 4. However, in contrast to cellularity data, on day 7, resultant PK3 scoring indicated increase inflammation above PLGA levels. Despite trends observed, histologically, there is very little variance and no statistical significance among experimental groups. In addition, as a result of the lungs being unperfused, large populations of red blood cells were also visualized (Figure 8).

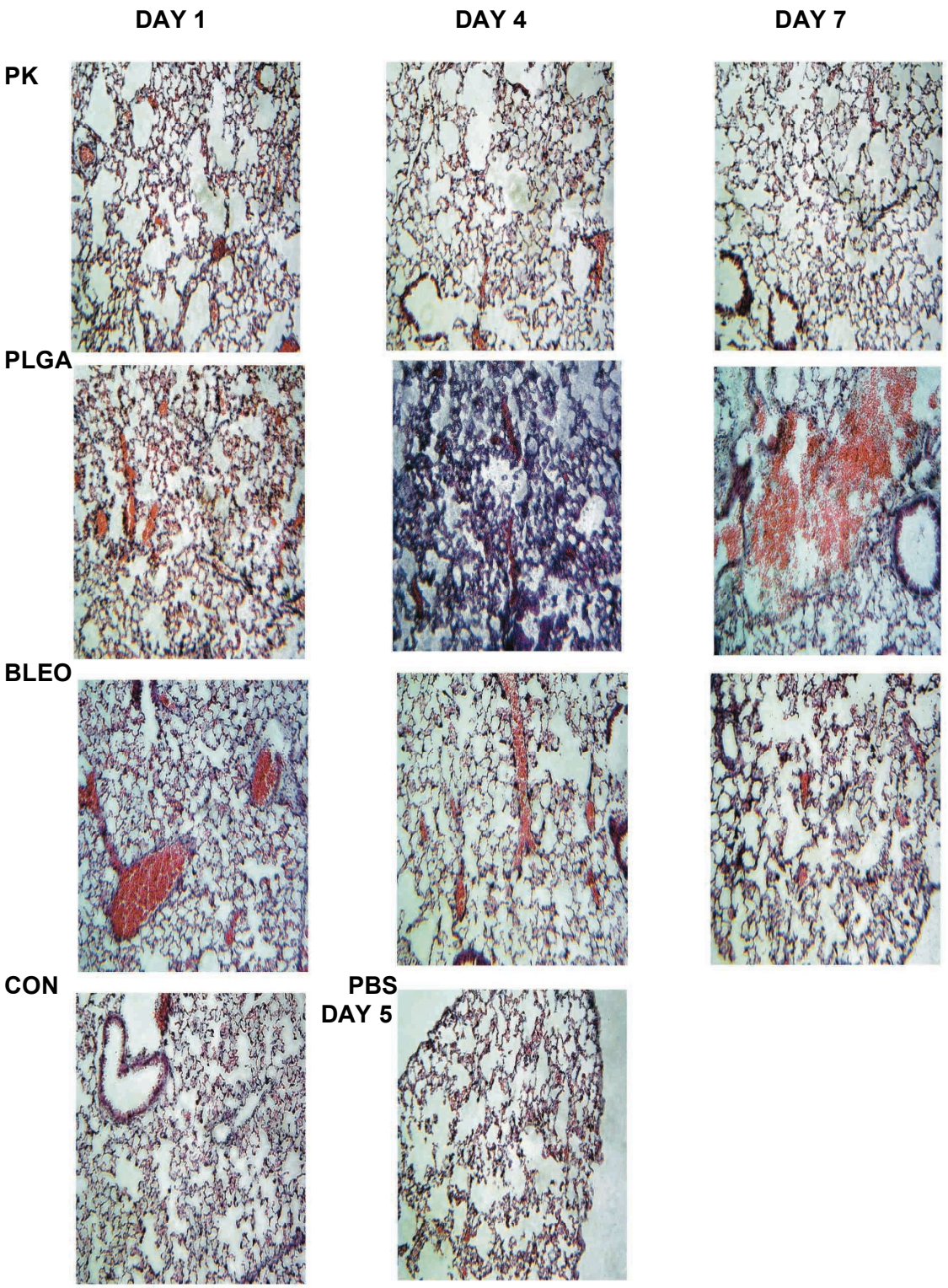

Figure 8. Histological Assessment of Particle Effect. Lungs were stained with H&E after intratracheal injections of 1.5 mg of PK or PLGA particles, bleomycin (BLEO), PBS, or no treatment (CON). PBS vehicle controls were sacrificed on day five.

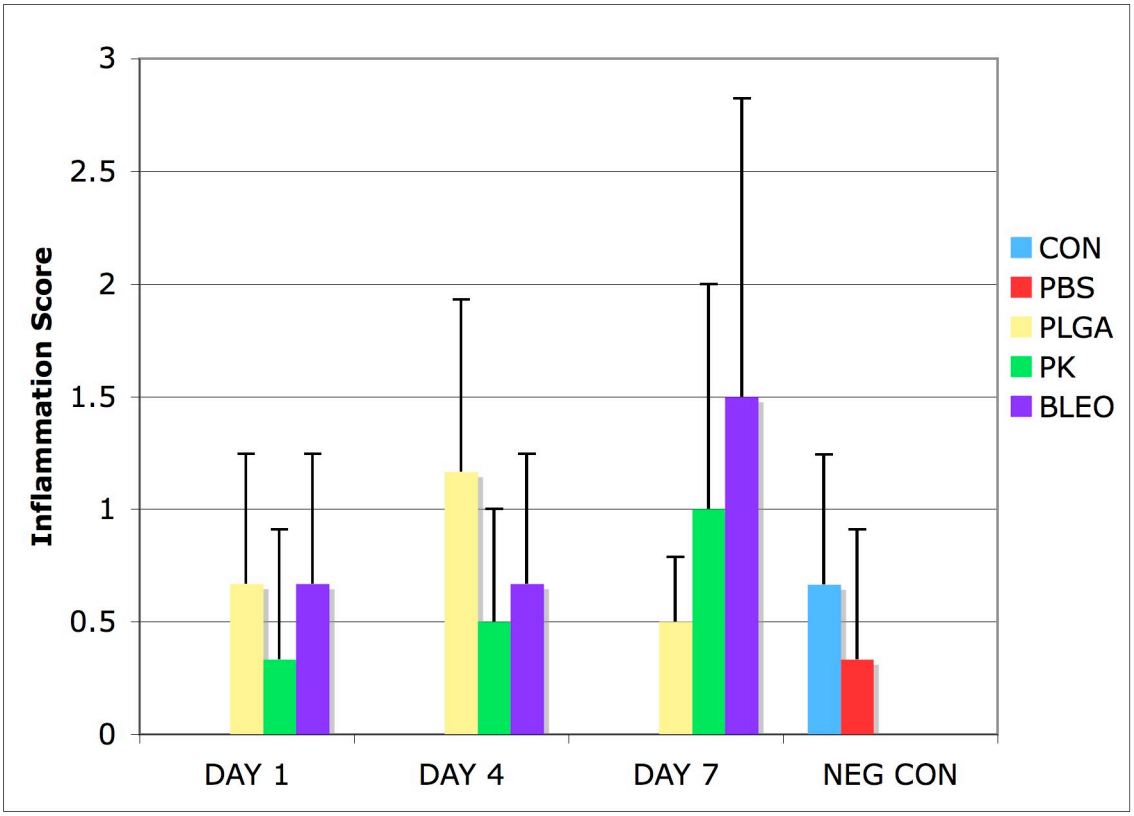

Figure 9. Histological Scoring After Intratracheal Particle Injections. Lungs were stained with H&E and scored after intratracheal injections of 1.5 mg of PK or PLGA particles, bleomycin (BLEO), PBS, or no treatment (CON). PBS vehicle controls were sacrificed on day five. Score scale (n=3): 0, no inflammation; 1, some inflammation; 2, more inflammation; and 3, most inflammation.

4.3.4 Cytokine Production in Response to Particles

U937 cells, stably transfected with an IL-1 luciferase reporter construct, were used to examine cytokine production in response to both PLGA and PK3 particles. We exposed cells to particles concentrations (approx. 0.07mg/well) identical to those used in our previous experiment investigating TGF-ß induced FN expression. Luciferase activity was normalized to total protein levels in each sample to account for minor well to well variations in cell numbers. Results indicated no significant increase in IL-1 expression due to either polymer formulation. By 48 hours, however, total IL-1 expression appears to diminish uniformly across samples. This reduction of expression coincides with observed contamination within the cell populations. We attempted to minimize risk of bacterial contamination; however, due to the non-sterile particle production conditions this was unavoidable. The particles and LPS were resuspended in initially sterile CellGro COMPLETE media, but the resuspension procedure was not performed aseptically. The inherent lack of sterility associated with the particles and procedure likely contributed to cell contamination and death leading to decreased detection of IL-1 expression (Figure 10).

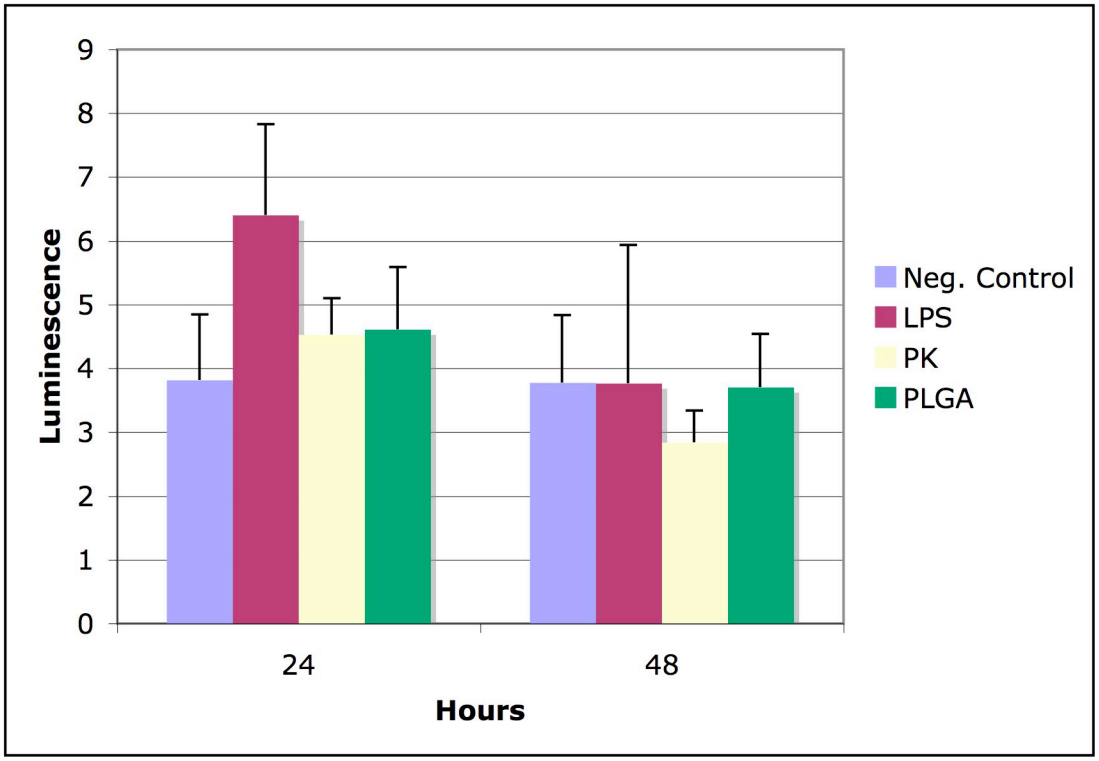

Figure 10. Particle Induced IL-1 Expression. U937 IL-1 luciferase reporter constructs were exposed to PLGA and PK3 particles at identical concentrations over 48 hrs. The controls included LPS as the positive and unstimulated cells as the negative. Luciferase activity was normalized to total protein amount in each sample.

4.4 Discussion

Pulmonary disorders marked by fibrotic scarring are intensified by inflammation. Therefore, it is essential to for any substance delivered to alveolar regions to minimize inflammation induction. To assess PKMs' viability as a small molecule drug delivery vehicle, empty PK3 particles as well as PLGA particles were synthesized according to aerodynamic design criteria. After injection of both polymeric particles into murine models, BAL fluid was analyzed for increases in inflammatory/immune cells. In addition a histological assessment was performed to determine any adverse particle influence.

We included PLGA in this study because it is one of the biomaterial standards of delivered microparticles. It is commonly used as a therapeutic carrier, but its applicability in pulmonary drug delivery is limited. In previous studies and in this current study PLGA induces significant inflammatory responses and possibly slight cell mediated immune activation. Macrophage populations illustrate significant ($p<0.001$) elevation from control groups at days 1, 4, and 7 due to PLGA particles. Macrophage influx by day 7 continues to trend upward, 3x above basal levels. Concurrently, at day 4 PLGA particles elicit minor lymphocyte influx, possibly indicating a cell mediated immune response to the particles. However, neutrophil populations were consistently elevated from basal levels, but not significantly.

In contrast to PLGA, PK3 injected particles inflamed lung tissue to a lesser degree. At day one, macrophage numbers remained similar to control values, by day 4 macrophage influx increase but to a lesser extent than PLGA groups ($p<0.01$). Macrophage infiltration subsided by day 7 closer to basal values ($p<0.05$); whereas, PLGA particles continued to induce macrophage influx on day 7. Lymphocyte values throughout the study remained comparable to control group levels, suggesting no cell mediated immune responses from PK3 particles. However, on day 1, neutrophil populations exhibited a slight increase from the control group, but returned to basal

levels by day 4 and 7. This indicates minor inflammation, but also demonstrated effective and rapid resolution.

In addition the histological examination of lung structures revealed minimal inflammation. Lung visualization and scoring appeared similar among experimental groups indicating no major histological changes due to the particles. This is consistent with previous studies. Typically, bleomycin induced histological lung alterations do not be come evident until day 8-10.

In vitro investigation of particle induction of IL-1 expression, an inflammatory cytokine, revealed insignificant IL-1 production. PLGA does appear to elicit more IL-1 expression than PK3, however differences are statistically insignificant. These results suggest that the particles, both PLGA and PK3, do not cause overproduction of inflammation facilitating cytokines. However, results may be skewed to due to the bacterial contamination observed by 48 hrs. It may be beneficial to develop a sterile particle synthesis technique or to produce particles in a sterile environment before repeating *in vitro* investigations on particles.

Overall, the most salient difference in cell populations for the two polymers was observed with macrophages. PLGA more efficiently activated inflammatory responses, which would be detrimental for pulmonary fibrotic disorders. Therefore, PK3 is a superior biomaterial for pulmonary applications. Although, PK3 elicits inflammatory responses distinctively elevated from basal levels, data indicates rapid resolution of the heightened inflammatory response. This distinguishes PK3 as an ideal candidate for a pulmonary drug delivery vehicle.

CHAPTER 5

CONCLUSIONS AND FUTURE WORK

5.1 Conclusions

Certain lung diseases characterized by excessive ECM deposition such as pulmonary fibrosis, have remained resistant to current treatments. These diseases are progressive in nature and likely require non-invasive therapy in order to halt or possibly reverse pathological alterations to the lung. Using polyketal microparticles as a drug delivery vehicle has the potential to expand non-invasive treatment possibilities. Through inhalation, novel therapeutic biomolecules can be encapsulated within polyketals and delivered non-invasively to alveolar regions of the lung.

The present study demonstrated that PK3 polyketal microspheres are an ideal therapeutic delivery vehicle for pulmonary applications due to its tissue biocompatibility. With inflammation facilitating fibrotic events prominent in many chronic lung diseases, tissue biocompatibility is an especially pertinent property. PK3 particles intratracheally injected into a murine model displayed limited inflammation induction based on BAL fluid cellularities. By day seven, following particle injections, macrophage, lymphocyte, and neutrophil levels were comparable to both the vehicle and unadulterated controls. However, the more commonly used biomaterial, PLGA, failed to clear inflammatory cells by day seven illustrating PK3's superior biocompatibility.

Furthermore, we have developed a particle synthesis procedure suitable for sufficient encapsulation of a small hydrophilic peptide. Through a solid in oil in water double emulsion technique, our model therapeutic attained load efficiencies translatable to clinical dosing requirements despite possessing little affinity for the hydrophobic polymer. In addition, this synthesis technique produced particles within the size constraints necessary for aerosolization enabling particles to be administered via

inhalation. However a major limitation of the particle synthesis procedure is it appears to render Ac-SDKP biologically inactive. The processing of loaded microparticles includes harsh chemical and mechanical manipulations that could affect the bioactivity of this particular peptide. Further studies will have to be performed to identify how the peptide is altered and where in the processing procedure alterations occur. With this data, restoration of processed Ac-SDKP bioactivity may be attainable.

5.2 Investigation of Ac-SDKP Bioactivity Loss After Processing

Our study revealed a significant loss of Ac-SDKP bioactivity ensuing encapsulation within PK3 microparticles. For Ac-SDKP to be an effective locally delivered anti-fibrotic to alveolar regions, it is imperative to elucidate the source of the peptide's inactivation. To identify the cause of Ac-SDKP dysfunction, we will isolate each step of the particle synthesis procedure and characterize its affect on Ac-SDKP. We will evaluate preservation of Ac-SDKP's chemical structure using mass spectroscopy. In addition, peptide bioactivity will be assessed through its efficacy in FN expression inhibition at each stage of the particle preparation protocol. Once we distinguish which particular particle synthesis manipulations inactivate the peptide, it may be possible to alter synthesis techniques or the peptide to restore activity.

5.3 Ac-SDKP Loaded Particle Reversal of Bleomycin Induced Fibrosis

Presuming a technique permitting Ac-SDKP encapsulation within PK3 microparticles preserving bioactivity is developed, we will investigate loaded microparticle efficacy in the prevention/ reversal of bleomycin induced pulmonary fibrosis. Using a murine model we will intratracheally administer empty polyketal microspheres, free Ac-SDKP, and Ac-SDKP loaded particles at day 0, 7, and 14 following fibrotic induction. At day 21 all mice will be sacrificed including vehicle, positive,

and negative controls and lungs assessed for fibrotic content. By performing a hydroxyproline assay on harvested lung tissue, ECM collagen content can be quantified and related to the extent of fibrotic progression. From this data, we can evaluate Ac-SDKP effectiveness, *in vivo*, on the reversal and prevention of fibrotic pulmonary disorders.

REFERENCES

2006. Lung Disease Data: 2006, American Lung Association, New York.

Arnold, M.M., et al., 2007. NanoCipro encapsulation in monodisperse large porous PLGA microparticles. Journal of Controlled Release, 121(1-2): 100-109.

Ashour, e.al., 2006. Bombesin Inhibits Alveolarization and Promotes Pulmonary Fibrosis in Newborn Mice. Am J Respir Crit Care Med, 173: 1377-1385.

Azizi, M., et al., 1997. High plasma level of N-acetyl-seryl-aspartyl-lysyl-proline: a new marker of chronic angiotensin-converting enzyme inhibition. Hypertension, 30(5): 1015-9.

Barnes, P., 2000. Mechanisms in COPD : Differences From Asthma. Chest, 117: 10S-14S.

Cashman, J.D., A.C. Eaves, and C.J. Eaves, 1994. The tetrapeptide AcSDKP specifically blocks the cycling of primitive normal but not leukemic progenitors in long-term culture: evidence for an indirect mechanism. Blood, 84(5): 1534-42.

Cavasin, M.A., et al., 2004. Prolyl oligopeptidase is involved in release of the antifibrotic peptide Ac-SDKP. Hypertension, 43(5): 1140-5.

Cavasin, M.A., et al., 2006. Therapeutic potential of thymosin-beta4 and its derivative N-acetyl-seryl-aspartyl-lysyl-proline (Ac-SDKP) in cardiac healing after infarction. Am J Cardiovasc Drugs, 6(5): 305-11.

Cavasin, M.A., et al., 2007. Decreased endogenous levels of Ac-SDKP promote organ fibrosis. Hypertension, 50(1): 130-6.

Crouch, E., 1990. Pathobiology of pulmonary fibrosis. Am J Physiol, 259(4 pt 1): L159-84.

Cryan, S.A., 2005. Carrier-based strategies for targeting protein and peptide drugs to the lungs. Aaps Journal, 7(1): E20-E41.

Crystal, R.G., V.J. Ferrans, and F. Basset, 1991. Biological basis of pulmonary fibrosis, in The Lung. Raven Press, New York, p 2031 pp.

Dailey, L.A., et al., 2006. Investigation of the proinflammatory potential of biodegradable nanoparticle drug delivery systems in the lung. Toxicology and Applied Pharmacology, 215(1): 100-108.

Edwards, D.A., et al., 1997. Large porous particles for pulmonary drug delivery. Science, 276(5320): 1868-1871.

Gauldie, J., et al., 2007. TGF-beta, Smad3 and the process of progressive fibrosis. Biochem Soc Trans, 35(pt 4)(661-4).

Gay, S.E., et al., 1998. Idiopathic pulmonary fibrosis: predicting response to therapy and survival. Am J Physiol, 157(4 pt 1): 1063-72.

Guo, e.al., 2004. Peroxisome Proliferator–Activated Receptor-. Diabetes, 53: 200-208.

Heffernan, M.J.a.N.M., 2005. Polyketal nanoparticles: A new pH-sensitive biodegradable drug delivery vehicle. Bioconjugate Chemistry, 16(6): 1340-1342.

Higashiyama, H., et al., 2007. Receptor-activated Smad localisation in bleomycin-induced pulmonary fibrosis. J Clin Pathol, 60(3): 283-9.

Hocevar, et.al., 1999. TGF-β induces fibronectin synthesis through a c-Jun N-terminal kinase-dependent, Smad4 independent pathway EMBRO, 18(5): 1345-1356.

Houchin, M.L., K. Heppert, and E.M. Topp, 2006. Deamidation, acylation and proteolysis of a model peptide in PLGA films. Journal of Controlled Release, 112(1): 111-119.

Jobe, A., 1999. The New BPD: An Arrest of Lung Development. Pediatric Research, 46(6): 641.

Kanasaki, K., et al., 2003. N-Acetyl-seryl-aspartyl-lysyl-proline inhibits TGF-beta-mediated plasminogen activator inhibitor-1 expression via inhibition of Smad pathway in human mesangial cells. Am Soc Nephrol, 14(4): 863-72.

Kasai, H., et al., 2005. TGF-beta1 induces human alveolar epithelial to mesenchymal cell transition (EMT). Respir Res., 6: 56.

Koslowski, R., et al, 2003. Evidence for the involvement of TGF-beta and PDGF in the regulation of prolyl 4-hydroxylase and lysyloxidase in cultured rat lung fibroblasts. Exp Toxicol Pathol, 55(4): 257-64.

Lee, S., et al., 2007. Polyketal microparticles: A new delivery vehicle for superoxide dismutase. Bioconjugate Chemistry, 18(1): 4-7.

Lombry, C., et al., 2002. Confocal imaging of rat lungs following intratracheal delivery of dry powders or solutions of fluorescent probes. Journal of Controlled Release, 83(6): 863-867.

Mapel, D.W., J.M. Samet, and D.B. Coultas, 1996. Corticosteroids and the treatment of idiopathic pulmonary fibrosis. Past, present, and future. Chest, 110(4): 1058-67.

Peltonen, et.al., 2004. Improved Entrapment Efficiency of Hydrophilic Drug Substance During Nanoprecipitation of Poly(l)lactide Nanoparticles. AAPS PharmSciTech, 5(1): Article 16.

Peng, H., et al., 2003. Ac-SDKP reverses cardiac fibrosis in rats with renovascular hypertension. Hypertension, 42(6): 1164-70.

Rhaleb, N.E., et al, 2001. Effect of N-acetyl-seryl-aspartyl-lysyl-proline on DNA and collagen synthesis in rat cardiac fibroblasts. Hypertension, 37(3): 827-32.

Schefe, e.a., 2006. Quantitative real-time RT-PCR data analysis: current concepts and the novel "gene expression's Ct difference formula. J Mol Med, 84: 901-910.

Selek, H., et al, 2003. Formulation and in vitro/in vivo evaluation of terbutaline sulphate incorporated in PLGA (25/75) and L-PLA microspheres. Journal of Microencapsulation, 20(2): 261-271.

Sheftel, V.O., ed., 2000. Indirect food additives and polymers, Migration and Toxicology. CRS Press, 219-220.

Springer, C., et al., 2005. Poly-lactic-glycolic acid microspheres: A biodegradable marker for the diagnosis of aspiration in hamsters. Pediatric Research, 58(3): 563-570.

Sung, J.C., B.L. Pulliam, and D.A. Edwards, 2007. Nanoparticles for drug delivery to the lungs. Trends in Biotechnology, 25: 563-570.

van der Meer, P., et al, 2005. Levels of hematopoiesis inhibitor N-acetyl-seryl-aspartyl-lysyl-proline partially explain the occurrence of anemia in heart failure. Circulation, 112(12): 1743-7.

Verrecchia, F.a.A.M., 2004. TGF-beta and TNF-alpha: antagonistic cytokines controlling type I collagen gene expression. Cell Signal, 16(8): 873-80.

Willis, B.C., et al., 2005. Induction of epithelial-mesenchymal transition in alveolar epithelial cells by transforming growth factor-beta1: potential role in idiopathic pulmonary fibrosis. Am J Pathol, 166(5): 1321-32.

Willis, B.C.a.Z.B., 2007. TGF-beta-induced EMT: mechanisms and implications for fibrotic lung disease. Am J Physiol Lung Cell Mol Physiol, 293(3): L525-34.

Yang, F., et al., 2004. Ac-SDKP reverses inflammation and fibrosis in rats with heart failure after myocardial infarction. Hypertension, 43(2): 229-36.

Yoshida, e.a., 2002. Monitoring changes in gene expression in renal ischemia-reperfusion in the rat. Kidney International, 61: 1646-1654.